The Pennsylvania State University

The Graduate School

Department of Electrical Engineering

DESIGN OF A SAFETY RADAR SYSTEM TO ENABLE SAFE OFF ZENITH LASER TRANSMISSION

A Thesis in

Electrical Engineering

by

James Yurack

Submitted in Partial Fulfillment
of the Requirements
for the Degree of

Master of Science

December 1994

We approve the thesis of James Yurack.

Date of Signature

C. Russell Philbrick Professor of Electrical Engineering Thesis Advisor	
Timothy J. Kane Assistant Professor of Electrical Engineering	
Larry C. Burton Professor of Electrical Engineering Head of the Department of Electrical Engineering	

Abstract

Powerful lasers are required in lidar experiments to obtain backscatter returns from various constituents in the atmosphere. Most lidar experiments take place in unrestricted airspace where aircraft could easily pass through the beam. The concern is for eye safety of the people on the plane who could look directly into the beam or those who may view a dangerous specular reflection off of an aircraft. Spotters are currently used in most lidar systems to watch for aircraft and shut off the laser if one approaches the beam. The spotter, however, cannot see through clouds to protect an aircraft from a laser that can scan down to a 30° elevation angle. In addition, the safety spotter must watch a larger portion of the sky in order to protect aircraft from the scanning beam.

A modified marine radar is presented as a primary safety system to help the spotter. A safety radar system is more reliable and is able to track with the movements of the WAVE-LARS scanning lidar system. The laser beam will be surrounded by the wide beam pattern of the radar. Through automated sensing circuitry, the radar can shut the laser off when aircraft approach the beam.

The marine radar is described along with the modifications made to it. The new safety radar system contains an improved transceiver housing, antenna, and a rack mounted electronics chassis which controls the safety radar from inside a mobile laboratory. Return signal plots are presented with analysis on why the system will be able to detect aircraft. Areas of future work are also proposed.

Table of Contents

List of Figures

List of Tables

Preface

This thesis describes why a radar system was chosen as the primary safety device for safe off zenith atmospheric laser transmission. Because the radar and laser used in this research both emit radiation which is capable of damaging body tissue, exposure limits and hazard areas around these sources were calculated for both and are listed in various tables in this thesis.

The exposure limits and hazard areas were calculated using set safety standards approved by the American National Standards Institute. All calculations are believed to be true using information gained from these sources. Therefore, the author assumes no responsibility for risk of loss incurred by the laser or radar systems described in this thesis.

I would like to thank my advisor, C.R. Philbrick, for his counsel during my graduate study at Penn State. He has helped me see how to tackle a problem and find all possible solutions for questions I might have. I would also like to thank T. Kane for his input on my research and what to look for in the future.

I would also like to thank the students with whom I have worked with in the past. Mike O'Brien, Sumati Rajan, Savy Mathur, George Evanisko, Paul Haris, Tim Stevens, Steve Sprague, Steve McKinley, Dave Machuga, Subha Maruvada, Brian Mathason, and Jim Anuskiewicz. They have helped me with my problems and have provided good times to be remembered. I shall miss them all.

Most people know that things will not get done without a good support staff. Glenn Pancoast, Tom Petach, Dan Lysak, Dave Blood, and Jim Jenness of the Applied

Research Laboratory along with Linda Kellerman, Julie Corl, and Bob Smith of the Electrical Engineering Department have helped me tremendously over the past two years with my research.

Lastly, I would like to thank my wife for putting up with my frustration during the writing of this thesis. Despite all of my stress, she always had a open ear to listen and arms to hold me. I love her dearly.

Chapter 1

Introduction

Many instruments use lasers in one way or another to track objects or remotely sense properties of the atmosphere. Laser remote sensing, or lidar, is similar to radar remote sensing except lidar uses light waves instead of radio waves. A laser sends out a pulse of light into the atmosphere where it scatters from the molecules and particles. The backscattered photons are collected by a receiver system from which information such as species type, density, size, and shape can be deduced. Through the use of pulsed lasers and time gating, range resolved measurements can be obtained on the atmospheric properties and can define the propagation conditions along the path.

1.1 The Problem

Because the number of received photons is determined by the backscattered intensity and the scattering in the atmosphere, powerful lasers are required to transmit a large number of photons. The energies in the lasers used for lidar systems are typically 1.2 to 1.5 J per pulse for Nd:YAG lasers operating at 1064 nm with peak power in excess of 200 Megawatts [1]. Two major hazards exist for lidar systems utilizing powerful lasers, one is electrical and the other is optical. The electrical hazard is primarily due to high voltages used to provide energy to the flash lamps, to control the Pockel cell, and to operate secondary emission multipliers. Electrical hazards are serious because of the potential for lethal shock. The electrical hazards in lidar use are mostly confined to a

protected area where trained operators are able to safely interact with the systems. Through safety interlocks and panic switches available on the system, the electrical hazard is easily controlled and monitored. In addition, precautions by trained personnel can insure safety when operating or working on high voltage systems. Training of all personnel in Laser and Electrical Safety, CPR, and Basic First Aid provides a final safety net for individuals working with lidar.

The optical hazards can occur in areas where a person could view a direct beam or glimpse at a specular or diffuse reflection. In addition, optical hazards include the possibility of the beam striking uncovered skin. The damage from optical hazards can result in blindness or irreparable skin damage. The optical hazards can occur in two regions, one is the local region which includes the laser and associated optics and the other is the volume of space where the beam is travelling through the measurement region. The beam usually encounters several optics or mirrors on the operating platform to direct it towards the atmosphere. When an optical device is moved or aligned, the chance of a dangerous reflection increases. Experienced personnel using safety goggles of a sufficient optical density can install beam stops to block unintended reflections when performing alignments or adjustments on the laser system.

The other hazard region is the atmosphere where the open path is of concern because aircraft can intercept the beam. The region of the atmosphere to be tested with a lidar system usually occurs in unrestricted air space. In other words, aircraft (military or civilian), hot air balloons, or gliders could be operating in or near a testing area. The concern is for eye safety of a pilot or passenger looking into the laser or a

person on the ground looking at a specular reflection off the aircraft. A direct view down the beam is a remote possibility in the vertically pointed case. Viewing a reflection off of a wing or fuselage, however, is more likely to occur and is more likely to be seen by people. Whether direct or from a reflection, the hazard is caused by an airborne object intercepting the laser beam. Notices to the Federal Aviation Administration, called Air NOTAMs (NOtice To AirMen), are used to alert pilots that lidar measurements are being taken in an area so pilots can alter their flight plans. However, there is no guarantee that a pilot has received the NOTAM or will plan to avoid the hazard area.

The current way to protect pilots and passengers in aircraft is to utilize safety spotters. Spotters are personnel who stand away from the lidar instrument (between 3 to 5 meters) and watch the volume around the laser beam. If an aircraft were to approach the beam, the spotter could shut the laser off until the aircraft passes.

The use of spotters is a temporary solution if regular measurements with a lidar system are to be conducted. Difficulties can arise from the alertness of the observer to the physical discomfort from cold or wet weather. Through exchanging the responsibility of watching for planes, spotters can help avoid optical hazards in the atmosphere.

With a static, zenith pointing lidar, the spotter need only concentrate on a small area around the beam since the only hazard is when the aircraft pass directly over the beam. If the lidar has an off zenith scanning capability, the spotter must be aware of a larger region of the atmosphere for aircraft. The problem is magnified when multiple

aircraft fly in the local vicinity. Furthermore, an aircraft behind a cloud or fog bank is still susceptible to a laser hit but cannot be detected visually by a spotter.

Since spotters cannot fully detect aircraft in poor weather conditions, an additional safety system must be developed to operate as an improvement in aircraft detection. This safety system must be reliable, able to operate in varying weather conditions, and be able to shut off the laser when an aircraft is headed towards the beam.

The proposed safety system is a modified marine radar with associated electronics to shut down the laser when an aircraft is in the vicinity of the laser beam. This safety system removes the optical hazards involved with using a lidar system in unrestricted air space by detecting aircraft independent of the use of spotters. In addition, this system can operate in varying weather conditions and requires little maintenance once the system is activated and set to the desired sensitivity. The idea of including a safety radar along with a lidar system has been used previously [2].

This thesis begins by presenting the scanning lidar for which the safety radar was built. The optical hazards of the laser are then calculated to show why this system was needed. Next, the marine radar and the modifications made to it are described in detail. Finally, a system analysis was performed to prove the safety radar will in fact help complement the spotter with aircraft detection.

1.2 The WAVE-LARS System

The safety radar system was developed for the Water, Aerosol, Vapor

Experiment - Lidar and Radar Sounder (WAVE-LARS), located at Penn State. WAVE-LARS represents a new generation of remote sensing instruments that will be used to help explore and record the properties of our changing atmosphere. WAVE-LARS, herein referred to as LARS, is a combination of three separate remote sensing instruments whose primary focus is to study the interactions of water vapor and aerosols around cloud structures. By understanding how clouds are formed and dissipated, we gain knowledge in the following areas: (1) the temperature and moisture structure needed to form or dissipate clouds; (2) dynamical processes taking place in clouds; (3) the radiative transfer process of the atmosphere.

The three remote sensing instruments that make up the LARS instrument are a scanning lidar system, a scanning radar system, and a static lidar system. Each of these systems are capable of measuring different properties that the others cannot detect. Bringing the three instruments together allows the user to compare or combine the results. In doing so, the LARS system becomes a powerful tool to study cloud physics and structure. LARS was designed to be portable and operate in most weather conditions to extend our knowledge by advancing the capability of remote sensing measurements. The abilities of LARS were first presented by Rajan et al. [3].

1.2.1 Scanning Lidar System

The scanning lidar system is illustrated in Figure 1.1. A Nd:YAG laser is used to transmit high intensity pulses at wavelengths of 1064 nm, 532 nm, and 355 nm. There are seven detectors used to receive the backscatter signals in the scanning lidar

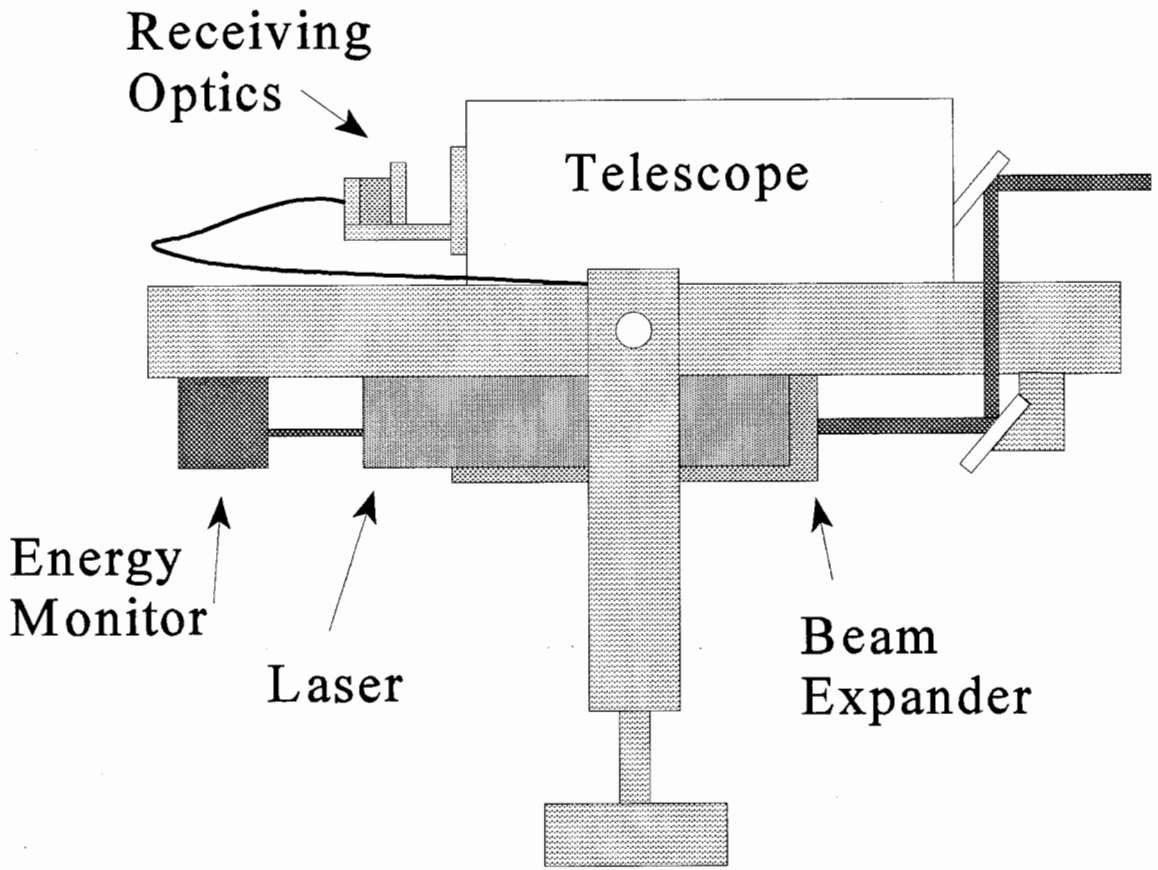

Figure 1.1 Side view of the LARS scanning lidar system. This figure shows the components on the scanning lidar system.

system. Six detectors are configured to measure the two backscatter components of polarization which are parallel and perpendicular to the transmitted wavelengths. The seventh detector is used to measure extinction in the atmosphere. From the variation of the nitrogen Raman scattered signal compared to the known uniform distribution of molecular nitrogen in the atmosphere, the optical extinction can be measured. The scanning lidar will be able to map the volume distribution of the aerosol concentration as well as detect regions where changes in their size and shape occur.

The scanning lidar is mounted on an optical table which is supported and allowed to pivot between elements in a reinforced aluminum fork. The lidar system is able to scan through the use of computer controlled stepper motors. From the computer, the type of scan, scan rate, and scan volume can all be determined through a computer program which drives the stepper motors [4].

1.2.2 Scanning Radar System

The scanning radar system, shown in Figure 1.2, uses a similar scanning platform as the scanning lidar system. The scanning radar transmits at 94 GHz, which was chosen because of its low atmospheric attenuation and its ability to measure the distribution of cloud droplets [5]. Since the wavelength of the 94 GHz radar is larger than most of the cloud particle sizes, the scattering from the cloud particles can be treated according to Rayleigh scattering theory. The radar produces a 3-D image of the small water droplets that make up clouds. From this information, cloud structure thickness and location can be mapped and studied. The scanning radar will be

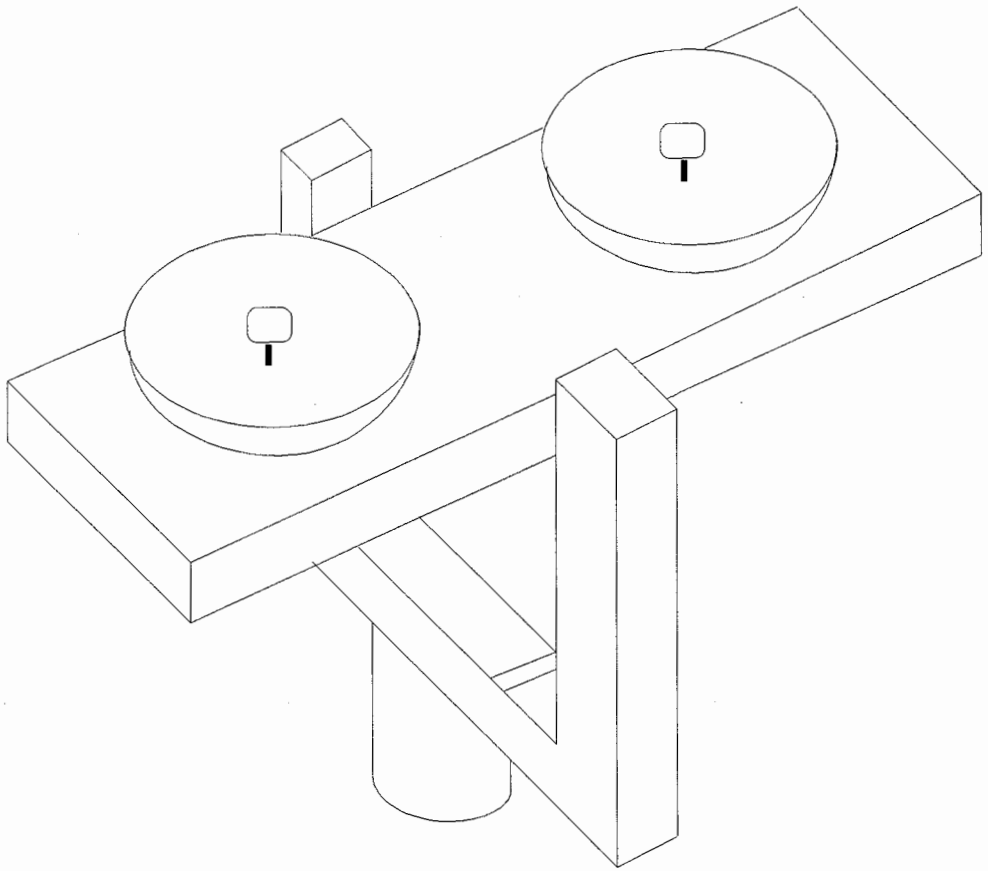

Figure 1.2 Scanning radar system for LARS. The scanning radar uses an identical platform as the scanning lidar.

programmed to track along with the scanning lidar so the same volume of space will be scanned at the same time.

1.2.3 Static Lidar System

The static lidar will be used to measure water vapor concentrations and temperature profiles along a chosen ray which is fixed for a particular experiment by using vibrational and rotational Raman scattering. The information gained on water vapor and temperature together with the information about particles and distribution of aerosols helps to understand the physics of how clouds are formed. The static lidar is the Penn State/ARL LAMP lidar system. Details about the LAMP lidar instrument have been reported in several places [6,7,8].

As of this writing, the scanning radar is still in the development stage. The fabrication of the scanning lidar has been completed and testing was initiated in the summer of 1994. Therefore, the acronym LARS will be used to describe only the scanning lidar system through the rest of this thesis.

Chapter 2

Optical Safety Issues In Lidar Use

To obtain useable signals from the backscattered radiation at altitudes above 60 km, powerful lasers are required. The operation of high power lasers requires that attention be given to safety for the system operators and others in the area of operation. Although administrative procedures, training, and safety plans can keep most laser hazards to a minimum for operations within the laboratory, other precautions must be taken in the regions where the beam propagates along an open path. To determine the optical hazards associated with lidar use, information about laser types and laser-tissue interactions must first be understood.

2.1 Laser Classification

There are three basic factors that determine a laser's ability to damage tissue and thus classify it for implementation of control measures. The three areas are: (1) the laser's capability to injure personnel; (2) the environment in which the laser is used; (3) the personnel who may use or be exposed to laser radiation. In area (1), laser characteristics such as wavelength, irradiance, exposure duration, and tissue affected are examined according to standards that determine the Laser System Hazard Classification to which it belongs. Areas (2) and (3) cannot easily be compared to a set of rules to determine the hazard classification. Although all three areas are considered, the classification is determined mostly from area (1) [9].

The classification of lasers is used to help the user determine what sort of control measures and safety requirements are needed when operating the device. The four classifications are described in Table 2.1.

Table 2.1 Laser System Hazard Classification [10]

Class I:	Laser is essentially safe and cannot emit harmful radiation levels for the maximum duration of the intended use. Control systems or surveillance is not needed.
Class II:	Laser is of low power (<1mW) and operating in the visible wavelengths (400-700 nm). The output is not intended to be viewed directly, but momentary viewing is safe before a normal aversion response (i.e. blinking) occurs.
Class III:	Laser is not safe for momentary viewing. The laser has the potential to cause injury if viewed with magnifying optics (Class IIIa). The laser will also damage tissue if viewed directly or after a specular reflection (Class IIIb).
Class IV:	Laser is hazardous to eye and skin tissue. Can cause materials to ignite. Laser is not to be viewed directly, through specular or diffuse reflections.

2.2 Laser Hazards to the Eye

There are many biological factors to consider in assessing where the most damage will occur and at what wavelength damage will occur to the eye. Since the eye is designed to be an optical detector, it is easy to see why the eye is of main concern when dealing with laser safety.

Figure 2.1 contains a side view of the eye. Light, upon entering the cornea, passes

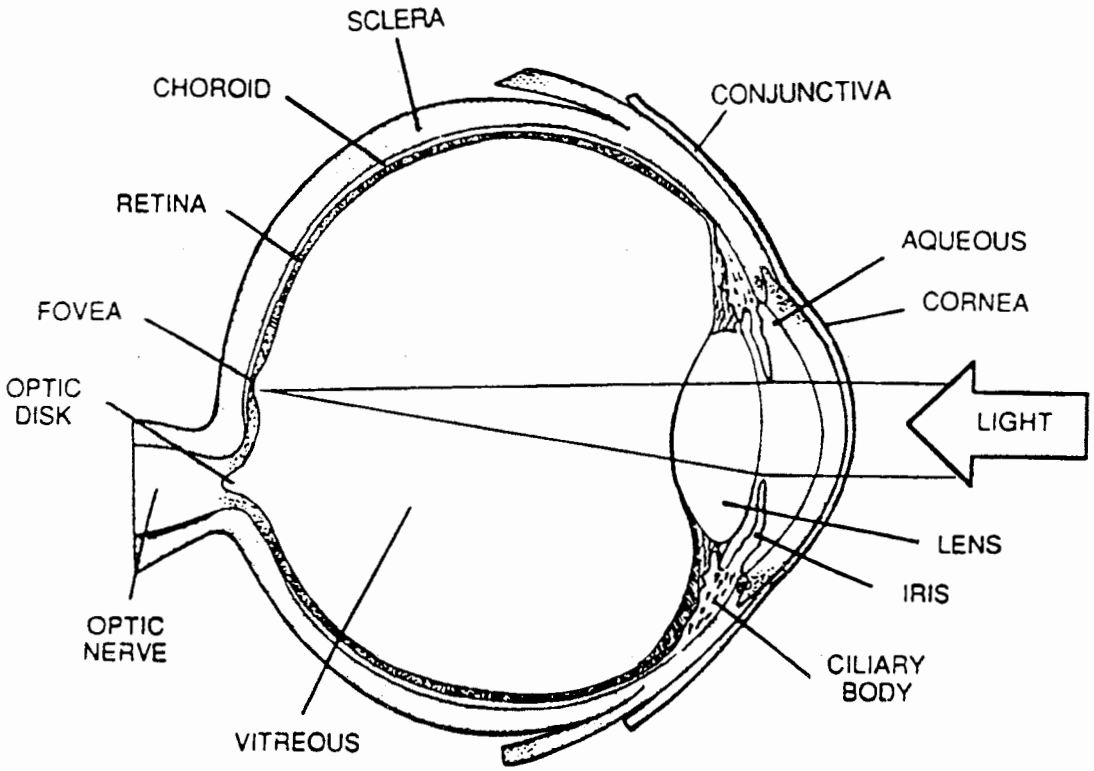

Figure 2.1 Anatomy of the eye [11]. Ultraviolet radiation is absorbed mostly by the lens while visible and near infrared are focused onto the retina.

through the aqueous humor, lens, and vitreous where it focuses on the retina. Not all incident light reaches the retina, however. Depending on the wavelength, light may be stopped by the cornea or may be refracted by the cornea and lens to be imaged on the retina [11]. The LARS lidar operates at three wavelengths covering the near IR, visible, and ultraviolet spectral regions.

2.2.1 355 nm Hazard

At the 355 nm wavelength of LARS, a small portion of the energy is absorbed by the cornea. Most of the energy is absorbed by the lens. A small fraction, about 2%, makes its way to the retina. A laser delivering hundreds of Megawatts in a small area will vaporize the tissue it strikes [12]. Short high intensity pulses at 355 nm can cause blast damage. In addition, the adverse effects that can occur from long exposures of low intensity 355 nm radiation include increasing the risk of developing cataracts. An important consideration at this wavelength would be the damage from photochemical reactions in tissues induced by the energy in the photons [13].

2.2.2 532 nm and 1064 nm Hazard

The other operating wavelengths, 532 nm and 1064 nm, are considered in the visible-near IR radiation category. Light in this region, 400-1400 nm, is the most sensitive part of the spectrum that the human eye can distinguish. Visible and near IR radiation pass through the cornea and lens where it is focused onto the retina. Since the focal point of the lens is 17 mm, light from a collimated source, such as a laser, enters

as parallel rays and is focused to a small bright spot on the retina. The effective irradiance of this point can be 10^5 times more than the irradiance incident on the cornea. The damage mechanism for visible and near IR radiation is heat. If the retina absorbs too much energy, the intense radiation can damage the light sensitive disks in the photoreceptors [10]. As in the case with the 355 nm wavelength, short high intensity pulses from the 532 nm and 1064 nm wavelengths deliver enough power to destroy and vaporize tissue at the molecular and cellular level [12].

2.3 Laser Hazard to Skin

It is usually forgotten that skin is susceptible to injury from laser radiation. Skin can easily sustain damage from a small exposure to intense radiation. Like the eye, the damage mechanism is thermal for most wavelengths but can involve photochemical damage with the shorter UV wavelengths. The skin, however, is not as susceptible to damage as the retina because there is no concentrator of the radiation, as in the case of the lens in the eye.

For skin, the absorption of energy is based on skin penetration and skin reflectance. In Figure 2.2, penetration depth for various wavelengths are described by the layer of the skin where the energy will be absorbed. The 532 nm and 1064 nm wavelengths can penetrate to the subcutis layer while 355 nm radiation will be stopped by the derma layer.

With high intensity pulses, a Nd:YAG laser can cause third degree burns to exposed skin. Over time, thermal damage to the deeper layers of the skin will occur in

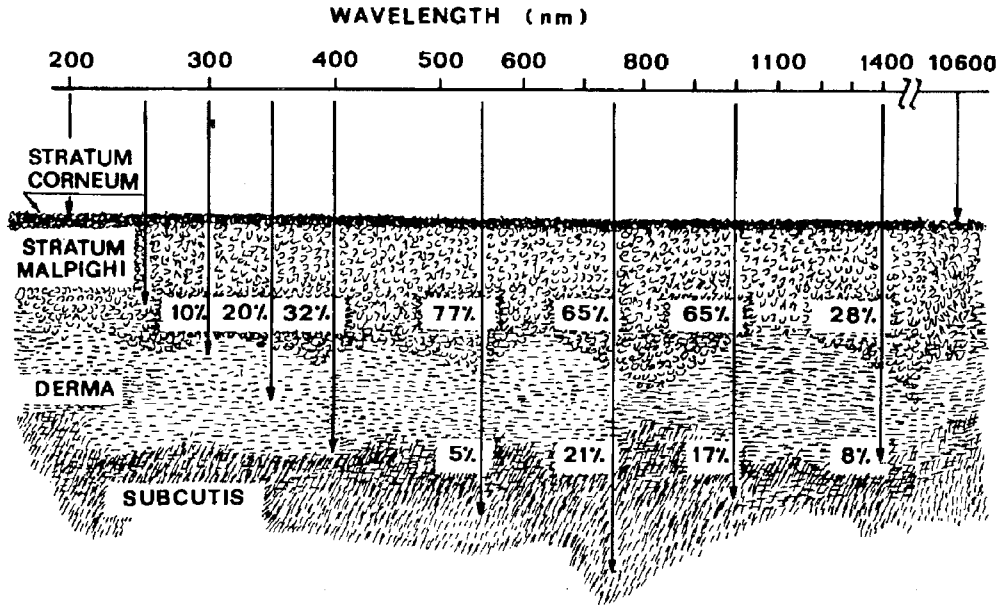

Figure 2.2 Skin penetration depths over several wavelengths [12]. The 532 nm and 1064 nm wavelengths are able to penetrate deeper into the skin than the 355 nm wavelength.

the affected area. Repeated exposures to UV radiation has been linked to accelerated skin aging and increased chance of skin cancer [12].

2.4 Analysis of the Optical Hazard for the LARS Laser

The optical hazard for the LARS laser can occur on the optical table or in the measurement region of the atmosphere. On the scanning platform, any unintended laser reflections must be handled with appropriate beam stops. Great care must be exercised during alignment procedures which must be carried out with the protective covers removed. During most operating periods, LARS personnel are not near the laser transmitter. However, during the alignment procedures, it is necessary to view diffuse reflections of the beam using protective eyewear. All watches, rings and other metallic or reflective materials must be removed before alignment activities begin. Because alignment procedures are done near the laser beam, the eye and skin are susceptible to damage. The optical hazards in the atmosphere include direct views or reflections of the laser off of aircraft. With aircraft usually flying thousands of feet above LARS, only the eyes of the pilot or passengers are susceptible to damage from the laser.

Using the American National Standard (ANSI Z136.1-1993), the Maximum Permissible Exposure (MPE) has been prepared for direct and diffuse viewing of the beam. The calculations for the MPE have all been based on a dark adapted open eye pupil diameter of 7 mm. Table 2.2 contains manufacturer specifications for the LARS laser where the three wavelengths are output on the same optical axis. Included in the

analysis is the MPE before and after the beam enters a 6X beam expander.

Table 2.2 LARS Laser Specifications [14]

Continuum Surelite II-20	Before Beam Expander	After Beam Expander
Energy @ 1064 nm	500 mJ	500 mJ
@ 532 nm	225 mJ	225 mJ
@ 355 nm	90 mJ	90 mJ
Beam Diameter	7 mm	42 mm
Beam Divergence	0.6 mrad	0.1 mrad
Pulse Width @ 1064 nm	5-7 nsec	5-7 nsec
@ 532, 355 nm	4-6 nsec	4-6 nsec

2.4.1 Intrabeam Viewing

The maximum permissible exposure (MPE) for the laser is a limiting energy density for incidence on the cornea. This density is a level to which tissue can be exposed without any hazardous effects. MPE is affected by exposure time, wavelength, number of exposures, and viewing angle. One such viewing angle is a direct look at the beam. Figure 2.3 shows the definition of intrabeam viewing with beam diameter, a, beam divergence, ϕ, and the distance, r, between the laser and eye. This viewing geometry is the most hazardous. Table 2.3 contains the MPE for the three wavelengths LARS will use for intrabeam viewing of a single pulse. As mentioned earlier, these are the limits of which the eye can absorb energy without harm. The 355

nm wavelength has a higher MPE because the eye does not focus the light into the retina, but rather the energy is absorbed by the cornea and lens.

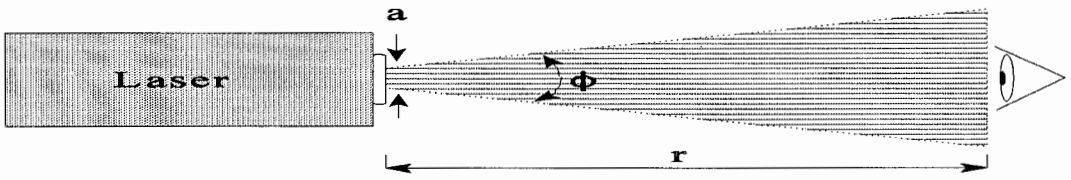

Figure 2.3 Definition of intrabeam viewing [9]

Table 2.3 Single Pulse MPE for Intrabeam Viewing of LARS Laser [9]

Wavelength	MPE (J/cm^2)
1064 nm	5×10^{-6}
532 nm	5×10^{-7}
355 nm	4.71×10^{-3}

The LARS laser transmits pulses at 20 Hz, which requires that the susceptibility to damage from multiple exposures be considered. If a beam was to enter the eye, reflexive aversion will limit the exposure to 0.25 seconds for visible and 10 seconds for IR radiation. To determine the multiple pulse MPE for the infrared and visible, the number of pulses at each wavelength is raised to the negative quarter power ($n^{-1/4}$, where n is the number of pulses) and multiplied to the single pulse MPE.

For UV light, special considerations must be made for determining the multiple pulse MPE. Since the body has no aversion response time to UV, a person cannot determine when their eyes or skin is being irradiated. The first signs of exposure do not show up immediately after irradiation but usually hours later. With repeated exposures to UV light, the effects are additive over a 24 hour period. Since the 355 nm beam must be transmitted simultaneously with the 532 nm beam, the single pulse MPE of the 355 nm beam can be divided by the number of pulses transmitted in 0.25 seconds. The multiple exposure MPE for all three wavelengths can be found in Table 2.4.

Table 2.4 Multiple Pulse MPE for Intrabeam Viewing [9]

Wavelength	MPE (J/cm^2)
1064 nm	1.33×10^{-6}
532 nm	3.34×10^{-7}
355 nm	9.42×10^{-3}

2.4.2 Nominal Ocular Hazard Distance

It is usually helpful to determine what the radiant exposure of the beam would be at a particular distance. The laser range equation can determine just that. The laser range equation divides the total power of the beam at some distance by the total area. The equation is,

$$H = \frac{1.27Qe^{-\mu r}}{a^2 + r^2\phi^2}$$

where, H - Radiant exposure (J/cm^2),

Q - Beam energy (J),

μ - Atmospheric attenuation coefficient (cm^{-1}),

r - Range (cm),

a - Beam diameter (cm),

ϕ - Beam divergence (radians).

If the atmospheric attenuation coefficient was assumed to be negligible (perfect transmission), then the laser range equation can be written as the Nominal Ocular Hazard Distance (NOHD),

$$NOHD = \frac{1}{\phi}\sqrt{\frac{1.27 * Q}{MPE} - a^2}$$

For the NOHD, the MPE to be used should be the multiple pulse intrabeam MPE, which would provide the worst case NOHD. Table 2.5 shows the NOHD for the LARS laser. As can be seen from the table, the NOHD increases after the beam expander. Even though the energy is spread over a larger area, the collimation properties of the beam expander make the beam dangerous for many kilometers.

Table 2.5 Nominal Ocular Hazard Distance for the LARS Laser

Wavelength	Before Beam Expander	After Beam Expander
1064 nm	11.52 km	69.1 km
532 nm	15.42 km	92.49 km
355 nm	0.183 km	1.02 km

2.4.3 Specular Reflections

Specular reflections occur when the beam reflects off of an object and maintains its collimation qualities. Specular reflections are dangerous because the beam's collimation is unchanged and it could be as hazardous as the direct beam. Figure 2.4 is an example of a specular reflection. For laser safety, specular reflections are treated as intrabeam viewing.

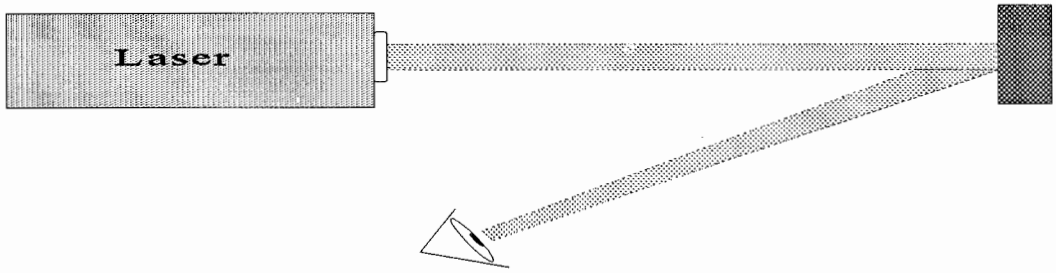

Figure 2.4 Intrabeam viewing of a specular reflection [9]

2.4.4 Nominal Hazard Zone for Diffuse Reflections

With most lasers, viewing a diffuse reflection is safe because the spatial distribution of the beam is reflected in 2π steradians by the illuminated surface. However, Class IV lasers are capable of delivering enough energy per pulse to make even diffuse reflections dangerous. A diagram of a diffuse reflection can be seen in Figure 2.5.

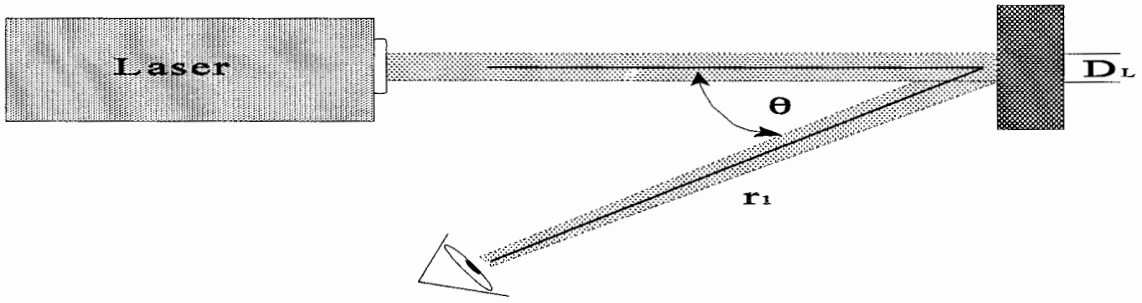

Figure 2.5 Intrabeam viewing of a diffuse reflection [9]

The method of calculating the safe distance to view a diffuse reflection can be taken from the following formula,

$$Q = \frac{\pi * MPE * [r_1 + \frac{D_L}{2}]^2}{\rho \cos\theta}$$

where, r_1 - Range from illuminated surface to eye (cm),

D_L - Diameter of beam at distance r (cm),

ρ - Reflectivity of surface at wavelength λ,

θ - Viewing angle.

Based on assumptions that $r_1 >> D_L$, the MPE for a diffuse reflection can be rewritten as,

$$MPE = \frac{\rho Q \cos\theta}{\pi r_1^2}$$

The nominal hazard zone for diffuse reflections can be written as,

$$NHZ = \sqrt{\frac{\rho Q \cos\theta}{\pi * MPE}}$$

The nominal hazard zone is an area that would be hazardous viewing from a Class IV laser on a diffuse reflective surface. This zone is illustrated in Figure 2.6.

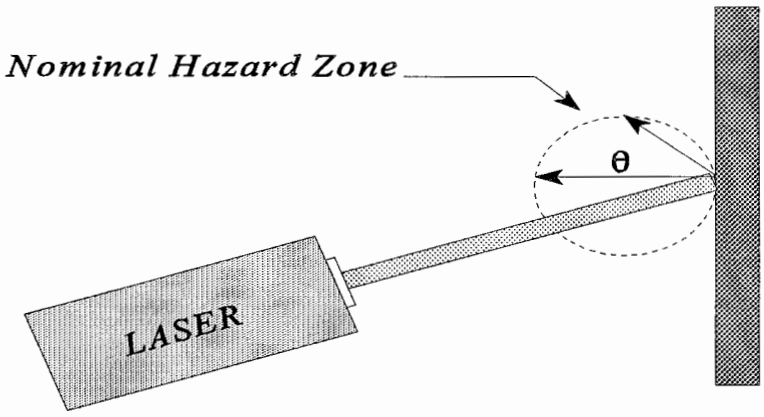

Figure 2.6 Nominal hazard zone for diffuse reflections [9]

For a worst case assumption with the LARS laser, it is assumed that the off axis viewing angle, θ, is zero and the reflectivity of the illuminated surface is equal to one. The nominal hazard zone equation reduces to,

$$NHZ = \sqrt{\frac{Q}{\pi * MPE}}$$

Using the multiple pulse MPE values for intrabeam viewing, the minimum safe viewing distance for a diffuse reflection from the LARS laser can be found in Table 2.6. Extended source criteria, if applicable, were taken into account when computing the nominal hazard zone.

Table 2.6 Safe Viewing Distance for Diffuse Reflecting Surface

Wavelength	Before Beam Expander	After Beam Expander
1064 nm	3.46 m	0.43 m
532 nm	4.61 m	0.076 m
355 nm	0.055 m	1×10^{-4} m

2.4.5 Skin Exposure Safety

To determine the MPE for skin, many factors are taken into account. As mentioned earlier, skin penetration by different wavelengths and skin reflectance do play a part. However, since skin comes in many different pigmentations, the ANSI standard assumes a worst case scenario where the skin reflectance is low. Thus, the

MPE becomes a factor of wavelength and exposure time. The MPE for skin is listed below in Table 2.7. The skin MPE is for exposure to both single and multiple pulses.

Table 2.7 Single and Multiple Pulse MPE for Skin [9]

Wavelength	MPE (J/cm^2)
1064 nm	0.1
532 nm	0.02
355 nm	4.71×10^{-3}

Taking the power at the exit aperture of the laser, the radiant exposure for all three wavelengths are hazardous to the skin before the beam expander. After the beam expander, the radiant exposure falls within safe levels for the 532 nm and 1064 nm wavelengths and does not pose a threat to skin. The 355 nm wavelength is still hazardous to skin after the beam expander. It must be pointed out that skin is a diffuse reflector. Even though the skin is safe, the radiation could be hazardous to the eyes of the person who is struck by the beam. Assuming that a person's hand is no more than 60 cm away from their eyes, the person could sustain damage to their eyes from the 532 nm radiation if the person were watching the point of illumination on their skin.

Chapter 3

Safety Radar System Considerations

In choosing a safety radar for LARS, several criteria had to be met. The three criteria by which the safety radar was chosen were operating frequency, overall size of the unit, and cost/availability of the radar. The system that was eventually chosen was the Raytheon Model R72 Raster Scan Marine Radar System from Raytheon Marine Company, Hudson, NH. This chapter describes why the system was chosen, the features of this system, and its limitations.

3.1 System Features

The R72 marine radar fit all of the criteria that was used in choosing a safety radar system. The operating frequency of the system, 9.4 GHz, suffers little attenuation by the atmosphere. In Figure 3.1, the absorption coefficient spectra for a range of Gigahertz frequencies from atmospheric species, rain, and fog are listed. The attenuation by atmospheric gases (mainly oxygen and water vapor) are near 0.01 dB/km for 9.4 GHz [15]. Figure 3.1 also shows that the calculated attenuation coefficient for clouds and fog is negligible at 9.4 GHz. This frequency allows penetration of clouds and fog banks to detect aircraft that may be directly behind them. Since spotters cannot see through clouds or fog, a radar operating at this frequency provides an additional safety element to complement the spotter.

The size of the R72 transmitter was another feature that fit well with the LARS

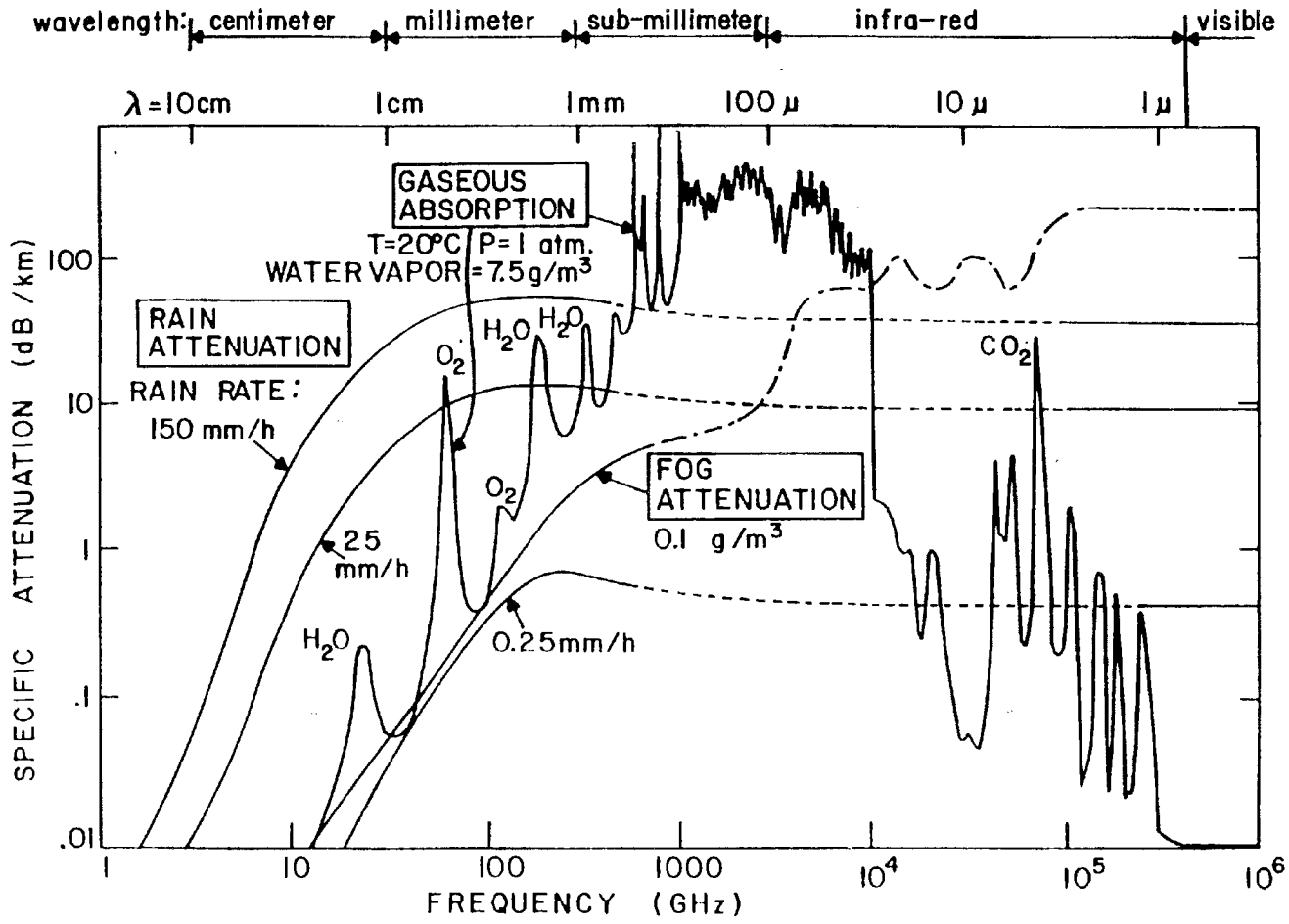

Figure 3.1 Atmospheric attenuation for Gigahertz frequencies. This graph shows the attenuation of various frequencies due to rain, gases, and fog [15].

system. Since the LARS table will scan volumes of the atmosphere, the radar transmitter and antenna had to either be co-located on the table with the laser or be a stand alone instrument that tracks the movements of the table and positions itself accordingly. A stand alone unit would be fairly large. In addition, the mechanics of having the lidar, 94 GHz radar, and safety radar all track to the same location at the same time would involve more motor controllers and computer memory to drive all these systems. The transmitter of the R72 is small enough that the unit can be mounted to the optical table.

The cost and availability of the R72 was another factor in choosing this system. Raytheon had this particular model on the shelf and was available for the money that was budgeted towards a safety radar. Moreover, the R72 has a proven track record when operated as a safety radar. A prototype safety radar design, utilizing a R72 system, was sent with the Penn State LAMP lidar system during the Point Mugu Measurements and Water Vapor Tests Campaign at Point Mugu Naval Air Station, Point Mugu, CA. U.S. Navy A-7 Corsair II aircraft performed 46 fly-bys over the LAMP system at varying altitudes which successfully demonstrated the safety radar shutting down the laser when the aircraft were in the field of view of the radar [16].

3.2 Marine Radar Specifications

The R72 radar system comes in two parts, a display monitor and scanner unit. The display monitor is of drip proof construction and is designed to be mounted overhead, on a wall, or on a table top. All functions are contained on a front panel display. A picture of the display monitor can be found in Figure 3.2. Specifications of the display monitor are

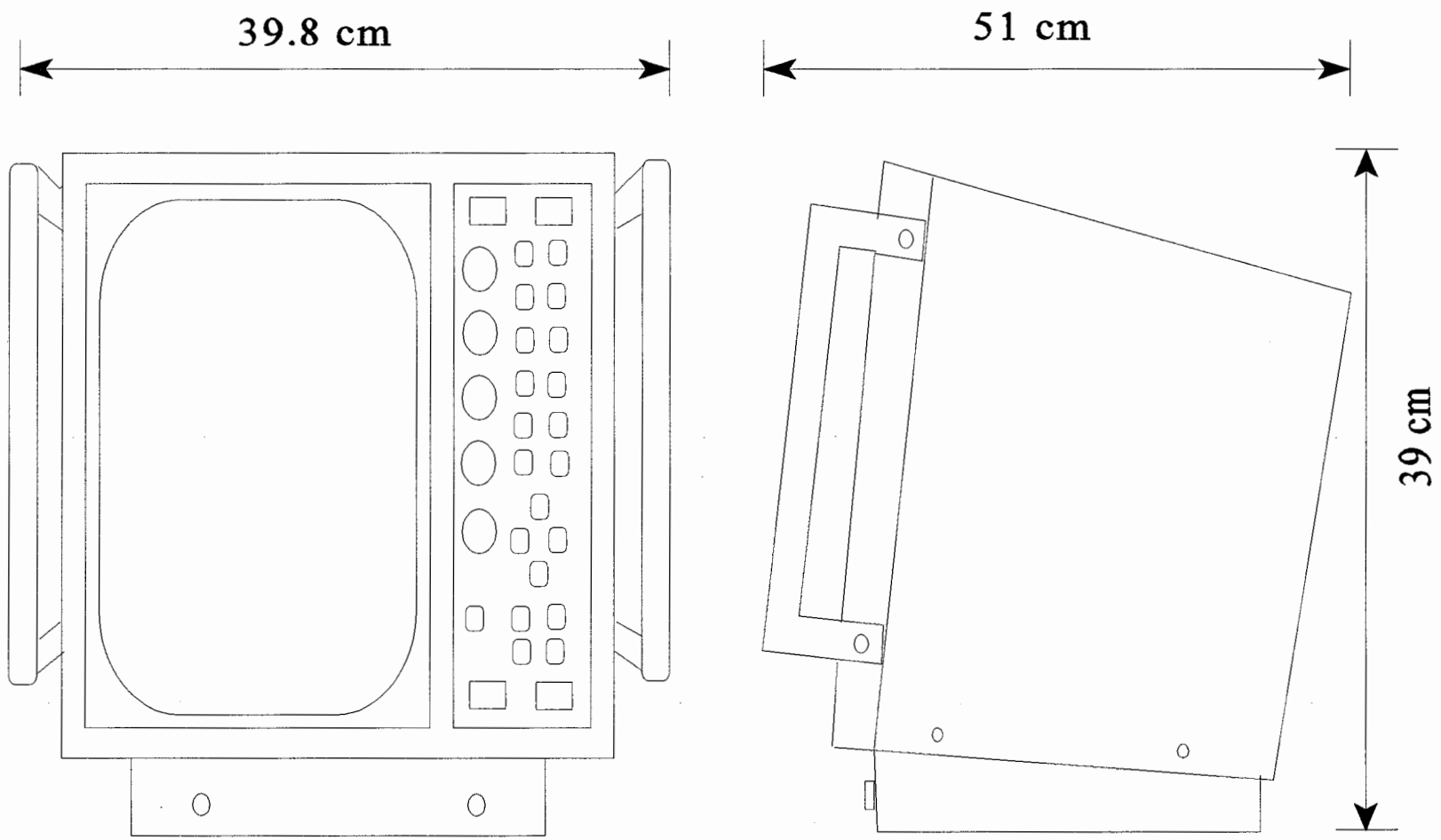

Figure 3.2 Raytheon R72 display monitor. The monitor's small size and accessible control panel allows it to be mounted in many places [17].

located in Table 3.1.

Table 3.1 R72 Display Monitor Characteristics [17]

Width	39.8 cm (15.67 in)	**Maximum Range**	72 nm
Height	39.0 cm (15.35 in)	**Minimum Range**	35 m
Depth	51.0 cm (20.08 in)	**Range Resolution**	< 30 m
Weight	18 kg (39.6 lbs)	**Bearing Resolution**	2.7° (w/3.5 ft array)
CRT	12" Monochrome	**Power Input**	12 VDC
Bearing	360° Graduated Scale	**Power Consumption**	120 W

The transmitter has a peak power of 10 kW with a linear receiver and an antenna drive motor. The scanner is connected to the display monitor by a single 10 meter long 20-pin conductor cable. The antenna array is 3.5 feet long and mounts above the scanner. The scanner is shown in Figure 3.3. Specifications are included in Table 3.2.

Table 3.2 R72 Scanner Characteristics [17]

Height	41.76 cm (16.44 in)	**Sidelobes**	less than -23 dB
Weight	24 kg (52.8 lbs)	**Transmitting Frequency**	9.410 GHz
Beamwidth (Horizontal)	2.4°	**Peak Power**	10 kW
(Vertical)	30°	**Rotation**	24 RPM

3.3 Marine Radar Limitations

The Raytheon R72 marine radar is a complete system that can easily fit the role of a safety radar for a lidar system. However, the R72 was not adaptable to the LARS

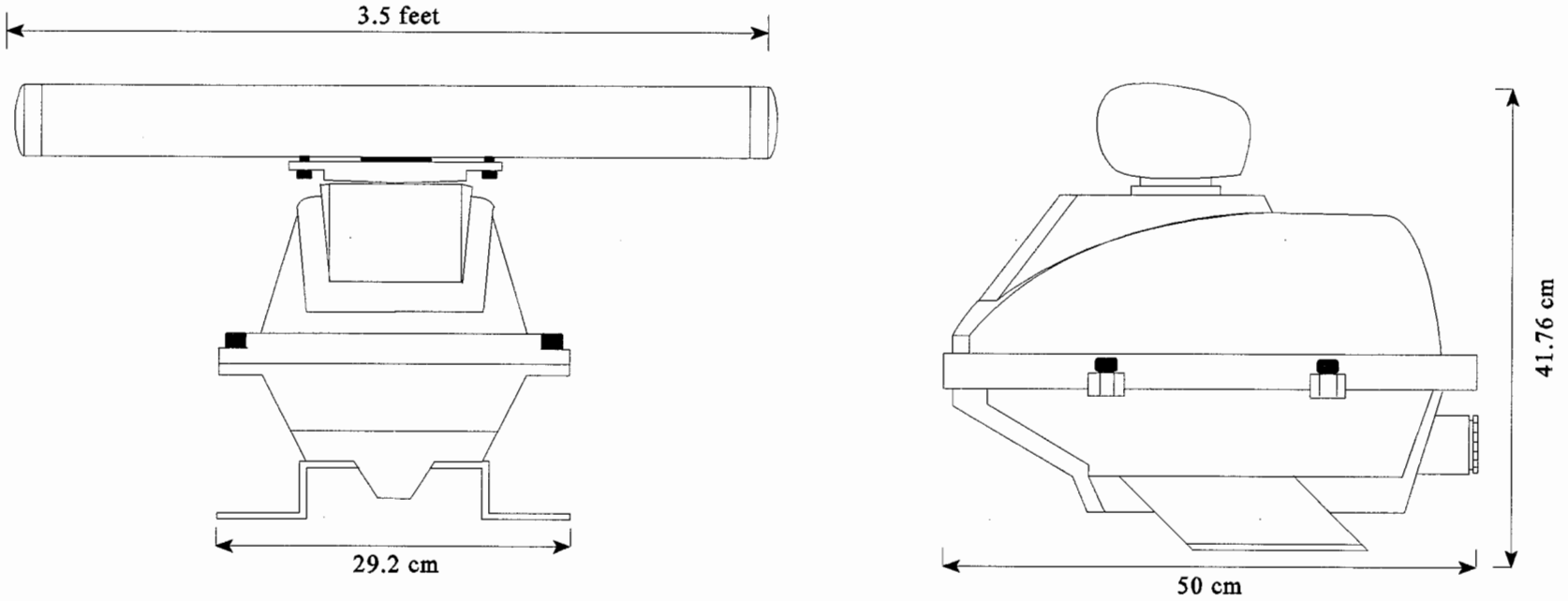

Figure 3.3 Raytheon R72 scanner housing. Shown are the front view and side view respectively [17].

instrument in its present form. Changes were needed in the antenna and scanner to fully integrate the R72 into LARS. For instance, the scanner is housed in a pedestal that weighs more than the table can withstand at the edge of the optical table. Due to the placement of the laser, beam steering optics and beam expander on the optical table, the weight of the transmitter had to be less than 50 pounds in order to keep the torque of the rotating table within the capabilities of the motors.

Similarly, the beam pattern produced by the original antenna array would not fully enclose the laser beam. The antenna array has a fan shaped pattern intended for horizon scans that distributes power over a large area. A more directive beam was required to protect an area around the laser beam.

Furthermore, the antenna array has a bearing motor mounted inside the pedestal which rotates the antenna to give the system a 360° field of view. If the antenna were held in place by disabling the motor, the system would shut down because the bearing pulse buffer circuit inside the display monitor is expecting signals from the antenna motor. When these signals are disrupted, the radar senses a problem and disables itself until the problem is corrected.

These limitations prevent the use of the R72 radar, in its present form, as a safety radar system. Through modifications, these limitations could be overcome. To this end, the following problems were addressed in order to integrate the R72 marine radar system into the LARS instrument: (1) decreasing the weight of the pedestal holding the scanner; (2) obtaining a smaller non-rotating antenna; and (3) removing the motor without disabling the system.

Chapter 4

R72 Radar System Modifications

By decreasing the weight of the scanner, using a different antenna, and removing the antenna motor, the R72 will be able to detect aircraft while mounted on the optical table. These three factors are the only changes needed to convert this marine radar into an aircraft warning device. In the LARS safety radar, several additional modifications were made on the R72 to give the radar a laser interrupt ability. A different monitoring system was incorporated into the modification plans to provide LARS with a more compact monitoring/control system for the safety radar. The first three sections of this chapter show how the R72 was converted from a marine radar into an aircraft detection device. The fourth section describes the laser cutoff circuitry which allows the radar to shut down the laser if it picks up a return signal from an aircraft. The fifth and sixth sections describe the custom made monitor and control panel for LARS.

4.1 Antenna

The antenna array that came with the marine radar produced a pattern with a narrow azimuth angle and a wide elevation angle. Since the radar must search an area around the laser beam, an antenna that produced a conical pattern centered on the laser beam was the logical step to replace the old array. Several antenna companies were contacted but only three were found to have antennas that were tuned for 9.4 GHz. The three antennas the companies offered were a horn antenna, a parabolic dish with

buttonhook feed, and a parabolic dish with central feed. Diagrams of each are found in Figure 4.1.

A parabolic dish antenna with a central feed system was chosen because of several advantages. The horn antenna was not chosen because it would protrude far enough off the optical table to prevent storage inside the LARS trailer. In addition, horn antennas were about three times more expensive and much heavier than parabolic dish antennas. A central feed system was chosen over a buttonhook feed due to possible problems in keeping the buttonhook feed aligned. The chosen antenna, a 15" parabolic reflector with 6" focal length, was purchased from Seavey Engineering Associates, Inc., Cohasset, MA. The specifications are given in Table 4.1.

Table 4.1 Antenna Specifications [18]

Frequency	9.4 GHz
Polarization	Linear, Manual Adjust
Gain	29.3 dBi
3dB Beamwidth	5.6°
Efficiency	60%

4.2 Motor Replacement Circuit

The antenna array on the original unit was designed to rotate in order to scan the intended area. The scan was accomplished by a motor installed in the scanner pedestal. Since LARS will not use a scanning antenna, the motor served no purpose and removing it

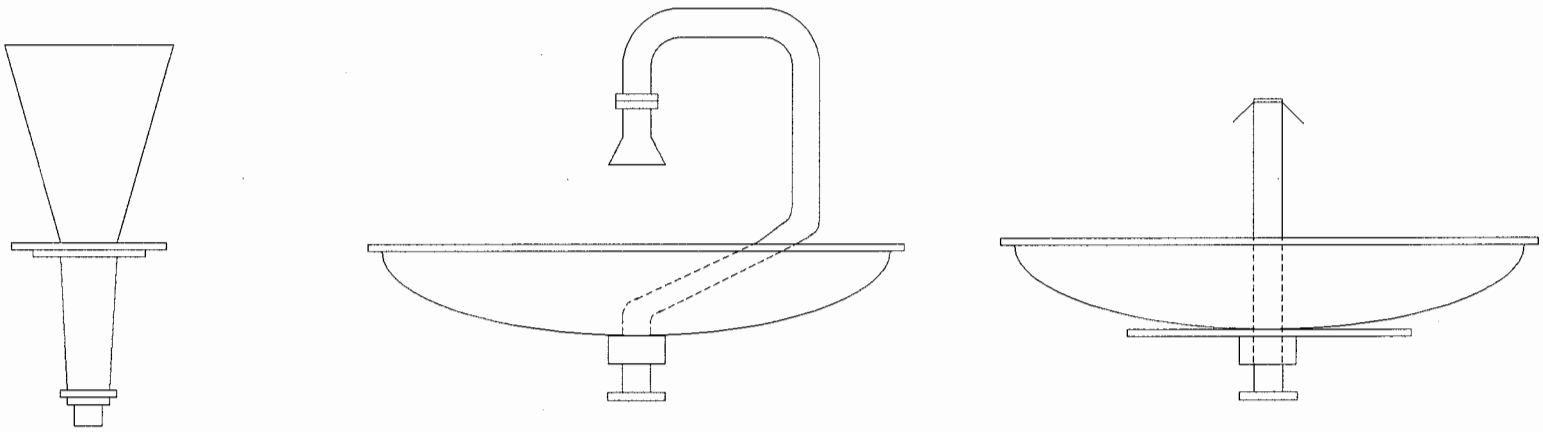

Figure 4.1 Antenna designs that were considered. From left to right; horn, buttonhook, center feed antenna.

reduced about 3.3 pounds from the total weight to be mounted on the optical table. However, removing the motor disabled the radar because the motor generated two signals important to radar operation. These two signals were a bearing pulse and bearing reset signal. The bearing pulse was used to synchronize antenna array rotations while the bearing reset was responsible for synchronizing the antenna with the display monitor. To solve this problem, a circuit was built that mimics the pulses of the motor encoder and sends it to the bearing pulse buffer on PC401, a printed circuit board, in the monitor unit. Since the output of the motor encoder was clock pulses with amplitudes of 5V, a timer IC that oscillates at the same frequency as the motor encoder would act as a perfect substitute.

The motor replacement circuit consists of a TTL 556 dual timer IC and a 7404 inverter IC. One half of the 556 is devoted to producing one pulse every 2.85 seconds for the bearing reset pulse while the other half produces a train of pulses to match the bearing pulse. Because of the nature of the bearing pulse and the limits of the time constants of the TTL 556, the output had to be inverted in order to match the output produced by the motor encoder. Figure 4.2 contains the circuit schematics of the motor replacement circuit. Figures 4.3 and 4.4 display the waveforms of bearing pulse and bearing reset respectively.

4.3 Scanner

In redesigning the scanner, the biggest factors taken into account were size and weight. A smaller unit would be easier for table placement. Without the motor, the

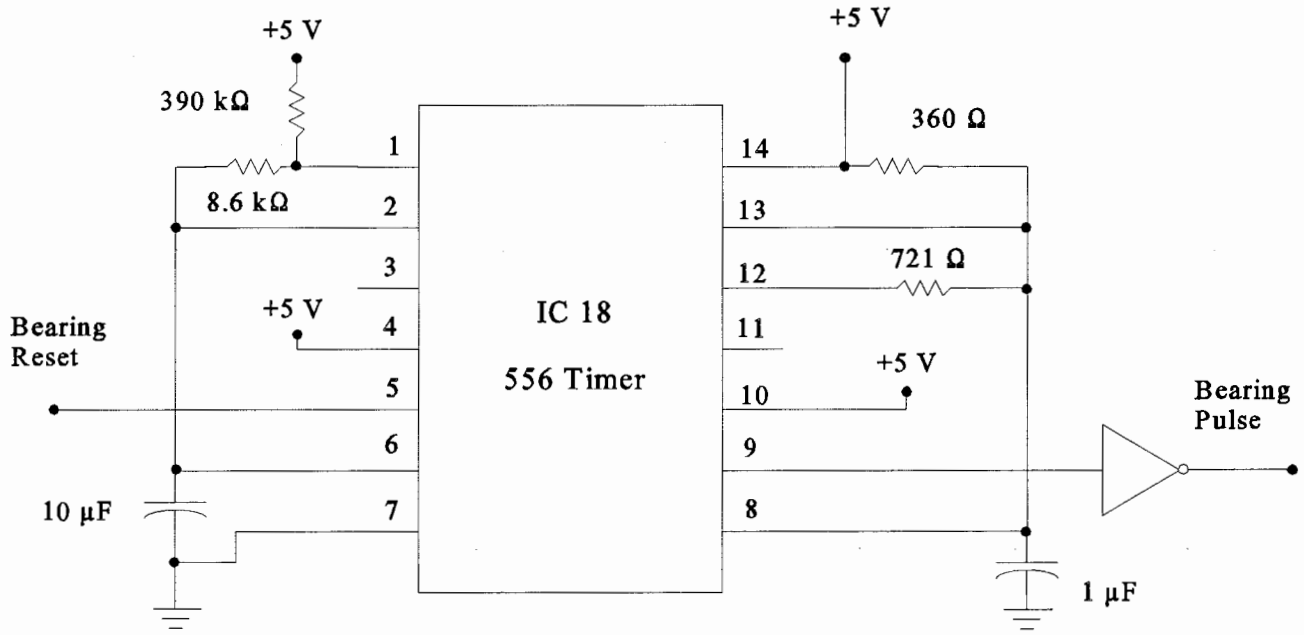

Figure 4.2 Schematic of the Motor Replacement Circuit. An oscillator was used to mimic the pulses of the motor to allow its removal from the scanner.

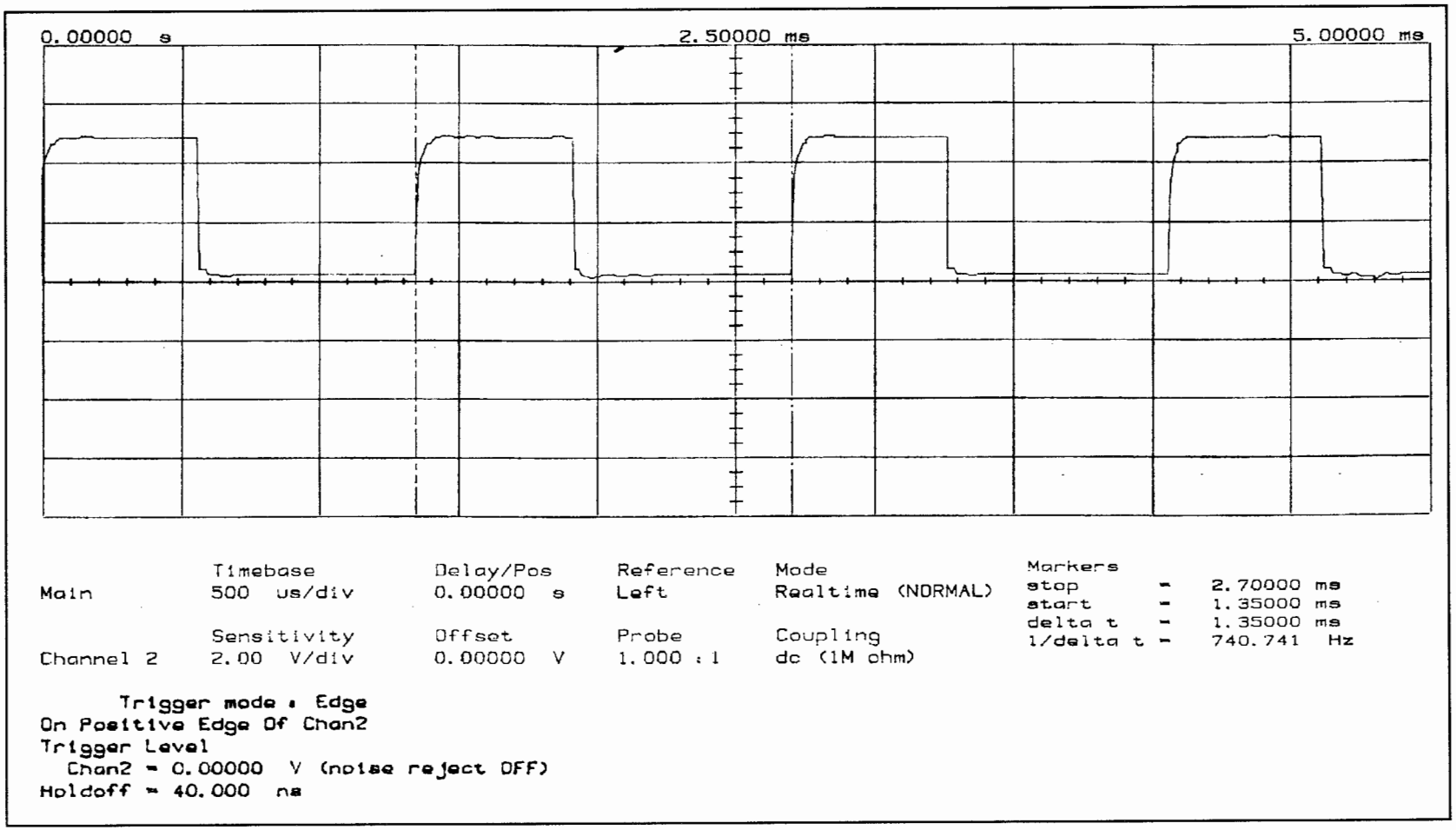

Figure 4.3 Bearing Pulse waveform. The bearing pulse was generated every 1.35 milliseconds.

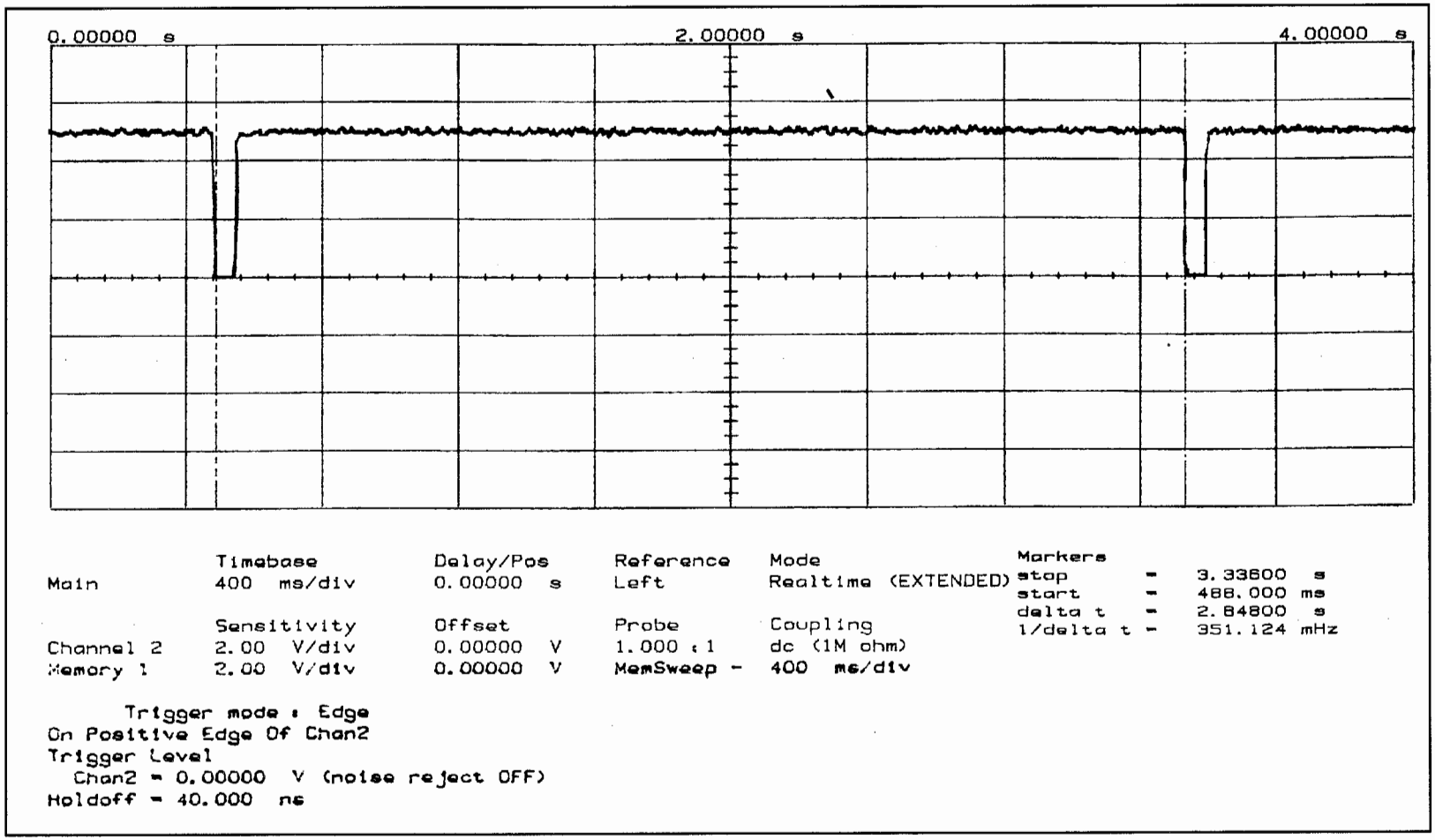

Figure 4.4 Bearing Reset waveform. The bearing reset was generated every 2.85 seconds.

scanner just barely falls within the weight limit for placement on the table. The scanner unit of the R72 radar contained the transmitter/receiver (transceiver), the motor, and circuit board CBD-941, a transfer point between the monitor and the transceiver. The motor has already been duplicated with the motor replacement circuit. This leaves the transceiver and CBD-941 inside of the scanner housing.

As mentioned earlier, the scanner housing without the motor weighs approximately 48 lbs, while the housing alone weighs 38 lbs. With a lighter housing, there would be less strain on the optical table stepper motors. In fact, if CBD-941 could be duplicated in a similar fashion as the motor replacement circuit, then a new scanner housing could just contain the transceiver.

Figure 4.5 shows a schematic of CBD-941. Most of the board is devoted to controlling the motor for the old antenna array. Since the motor has already been removed, the only functions left are connections from the terminal board, PC404, to the scanner. It would be easy to directly connect the interconnection cable to the scanner except for one IC on CBD-941. The IC, TL497ACN, is a switching voltage regulator. On this board, a +15V source from the monitor is inverted by this IC to -15V for use in the receiver. If -15V could be sent over the interconnection cable, then all of the wires inside the cable could be connected directly and CBD-941 could be removed.

It was discovered that pin 24 in the quick disconnect plug of the interconnection cable does not have a function. Pin 24 originates from the terminal board in the display monitor. By moving one wire on the terminal board, -15V will go to the receiver over the interconnection cable. Figure 4.6 shows the back side of the terminal board. This figure

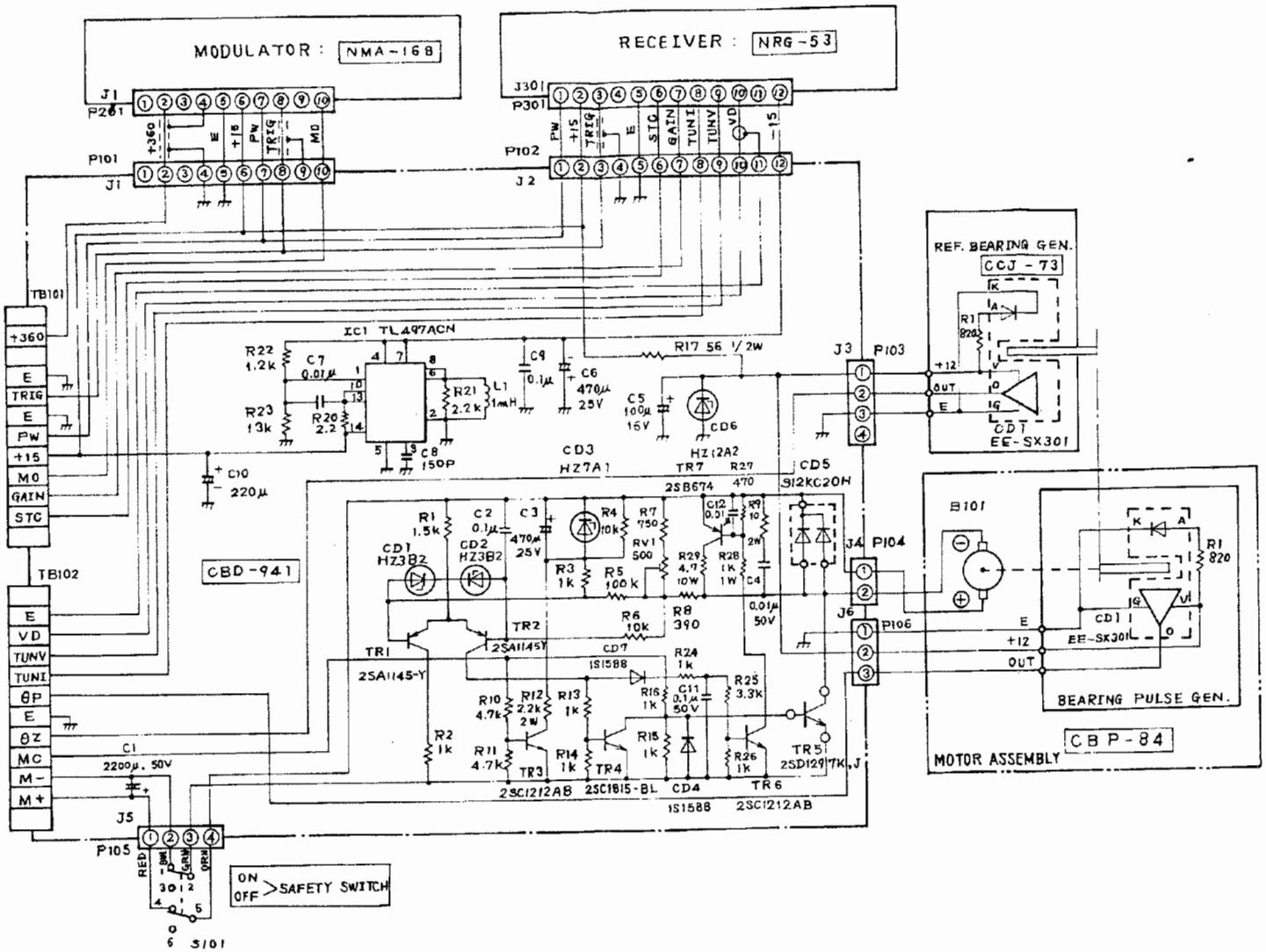

Figure 4.5 Circuit drawing of CBD-941 [17]. This circuit board was removed from the scanner housing when the functions of TL497ACN were duplicated and the bearing pulses of the motor were replaced with a timing circuit.

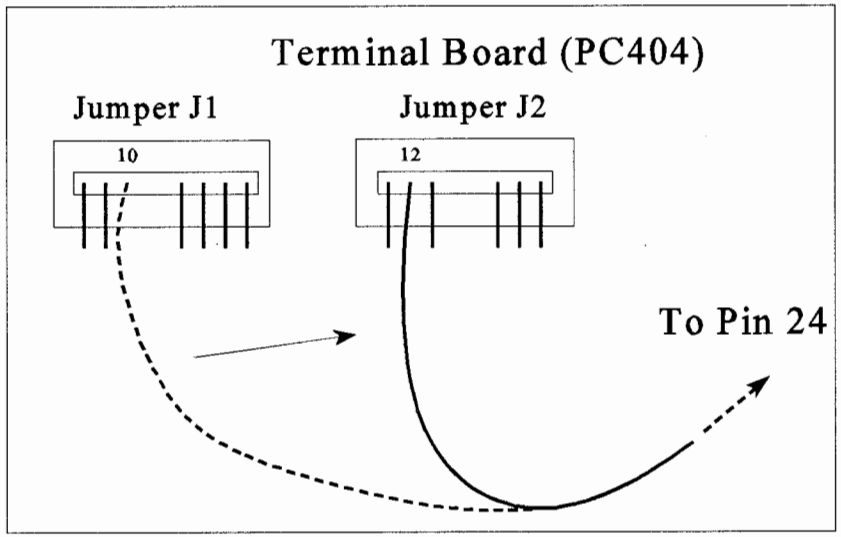

Figure 4.6 Terminal board of R72 radar. This figure shows how -15V was sent to the transceiver over the interconnection cable which led to the removal of CBD-941. This is the rear view where the interconnection cable connects to the terminal board.

shows exactly what was done to provide -15V over the interconnection cable. Several other lines in the interconnection cable were not used due to the removal of the motor. These lines were connected to TB101 and TB102 on Figure 4.5. The new wiring diagram of the quick disconnect plug is summarized in Table 4.2.

Table 4.2 Pin Wiring of the Interconnection Cable

1	+360V	7	*	13	TUNI	19	PW
2	E	8	VD	14	*	20	E
3	*	9	E	15	*	21	STC
4	*	10	+15V	16	*	22	E
5	TRIG	11	+15V	17	*	23	GAIN
6	E	12	TUNV	18	*	24	-15V

* - Not in use or not generated by the transmitter or receiver.

A new housing was built without CBD-941 that is smaller and lighter than the original unit using aluminum sheet. It measures 16.125" L x 8.75" W x 7" H. The transceiver sits upside down such that the waveguide is near the optical table. The transceiver is supported on three legs. The legs are bolted to a plate which is then bolted to the optical table. Thus, either the transceiver can be removed by itself or the table plate can be removed with the transceiver still attached. The new housing then bolts to the sides of the table plate. The housing has a notch cut for the waveguide to pass through. A rubber gasket seals the housing to the waveguide which makes the unit waterproof. The weight of the transceiver in the new housing is 16.9 pounds, a difference of 31.1

pounds. A sketch of the modified scanner housing can be found in Figure 4.7.

4.4 Laser Cutoff Circuitry

The modified radar now has the planned capability to sense aircraft. A circuit was needed to interrupt the laser pulses if a plane approaches the beam. William Moyer, an engineer with the Penn State Applied Research Laboratory, designed the first such laser cutoff device for the LAMP system [19]. The laser cutoff circuit was designed to produce a TTL level signal when a target enters the beam of the radar. This TTL signal would disable the laser's Q-switch until a manual reset switch was enabled.

The laser cutoff circuit for LARS is based on the original circuit meant for LAMP. The LARS circuit contains an additional safety interlock which the LAMP circuit does not possess. A wirewrapped circuit board was prepared and tested which includes a push button reset switch. The circuit can be divided into two subgroups for easier understanding of its makeup. The subgroups are a thresholding function and a blanking function.

The laser cutoff circuit works by reacting when a return signal crosses an operator set threshold. There is noise just after the radar fires a pulse which appears on the return signal channel. This noise is of a sufficient magnitude to cross the threshold every time the radar pulses. A blanking function is needed to bypass this noise so a false detection does not occur.

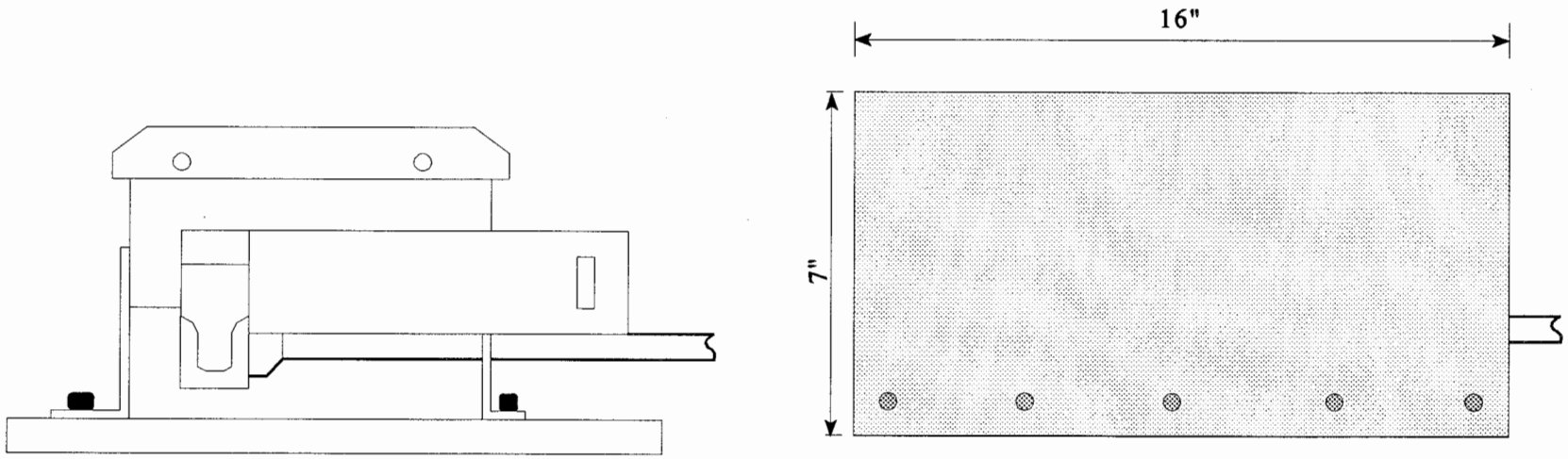

(a) (b)

Figure 4.7 Side view of the transceiver. Diagram (a) is the transceiver without the modified housing. Diagram (b) is the transceiver inside the modified housing.

4.4.1 Blanking Function

The blanking ability is needed to cover the region of noise remaining from the transmit/receive switching of the radar. The blanking function is a time delay that is used in conjunction with the radar timing signal, TRIG. When the transmitter fires a pulse, significant noise is created that appears on the video signal line, VD. VD is the line from the receiver which contains information on received signal strengths. VD is normally near zero volts and falls negative at the same time the pulse is transmitted. Because VD is used as a target indicator, the time after the switching noise is where aircraft returns will be detected. By blanking the laser cutoff at the time of pulse transmission, the noise pulse is effectively disregarded, thus eliminating false detection shutdowns from noise.

The blanking circuitry is drawn in Figure 4.8. As mentioned earlier, the blanking function uses the timing signal TRIG. TRIG will drop to -15V about six microseconds before transmitting a pulse. TRIG rises to +15V just before a pulse is generated. TRIG stays at +15V for 3 microseconds before settling to zero. The radar pulse is transmitted about 500 nanoseconds after TRIG rises to +15V.

TRIG is a signal input into a high speed voltage comparator, producing NLTRIG. As TRIG drops to -15V at the start of the cycle, NLTRIG drops low, holding a binary and decade counter in reset. When NLTRIG goes high, the binary counter increments by one every 500 nanoseconds, equivalent to 75 meters. This four bit binary counter sends its output to a binary comparator. The other signal sent to this binary comparator comes from a dipswitch package that can be set by the user. The dipswitch allows the user to set the desired blanking interval. The output of the binary comparator, DETEN (DETect

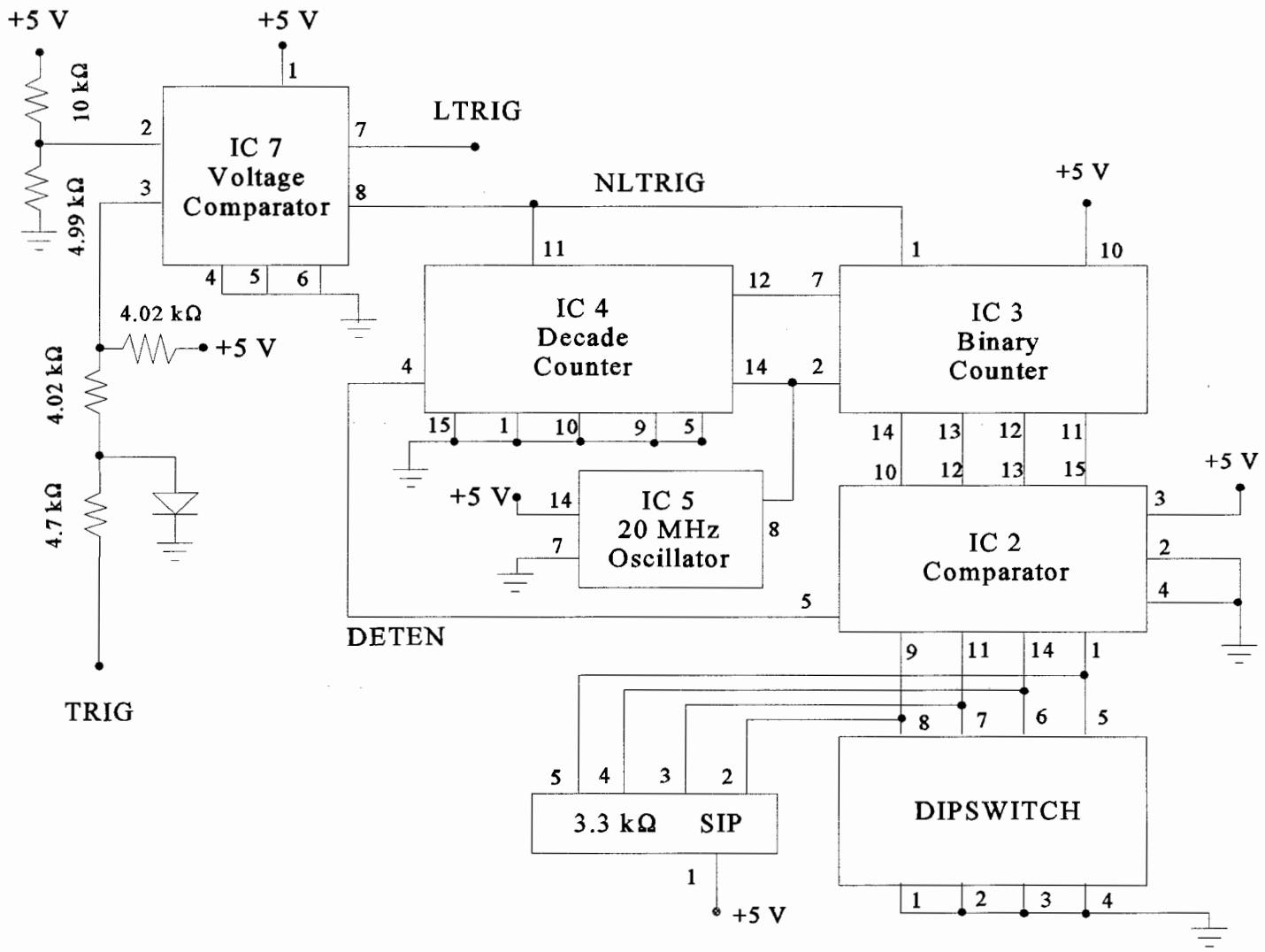

Figure 4.8 Blanking circuitry for laser cutoff. The blanking function is used to eliminate false detection shutdowns from the switching noise. Drawing is adapted from [19].

ENable), enables the detection circuitry to operate in the thresholding subgroup. DETEN is low until the binary counter registers a higher number than the user inputed blanking level. At this point, DETEN goes high allowing the cutoff circuit to operate. When DETEN goes high, further counting is stopped in the decade counter, thereby freezing the number in the binary comparator. The blanking function can be set by the user in intervals from 500 nanoseconds (all switches closed) to 7.5 microseconds (switches 2,3, and 4 open.) The blanking function cannot be set at 8 microseconds (all switches open) because the binary counter cannot count higher than 8 microseconds (see IC 2 and 3 in Figure 4.8.) Table 4.3 shows how much time is changed by toggling the respective switch. A timing diagram of TRIG, NLTRIG, VD, and DETEN is plotted in Figure 4.9.

Because DETEN disables the cutoff circuitry, a radar "hole" is created by which an aircraft can pass by undetected. However, aircraft must maintain a cruising altitude of no less than 1000 ft above the highest point over a populated area [20]. Since LARS will likely be tested near populated facilities, aircraft will typically fly above the hole created by the blanking circuitry and can thus be detected by the radar.

Table 4.3 DIPSWITCH Settings for DETEN

Base DETEN setting	500 nanoseconds
Open switch 1	+ 500 nanoseconds
Open switch 2	+ 1 microsecond
Open switch 3	+ 2 microseconds
Open switch 4	+ 4 microseconds

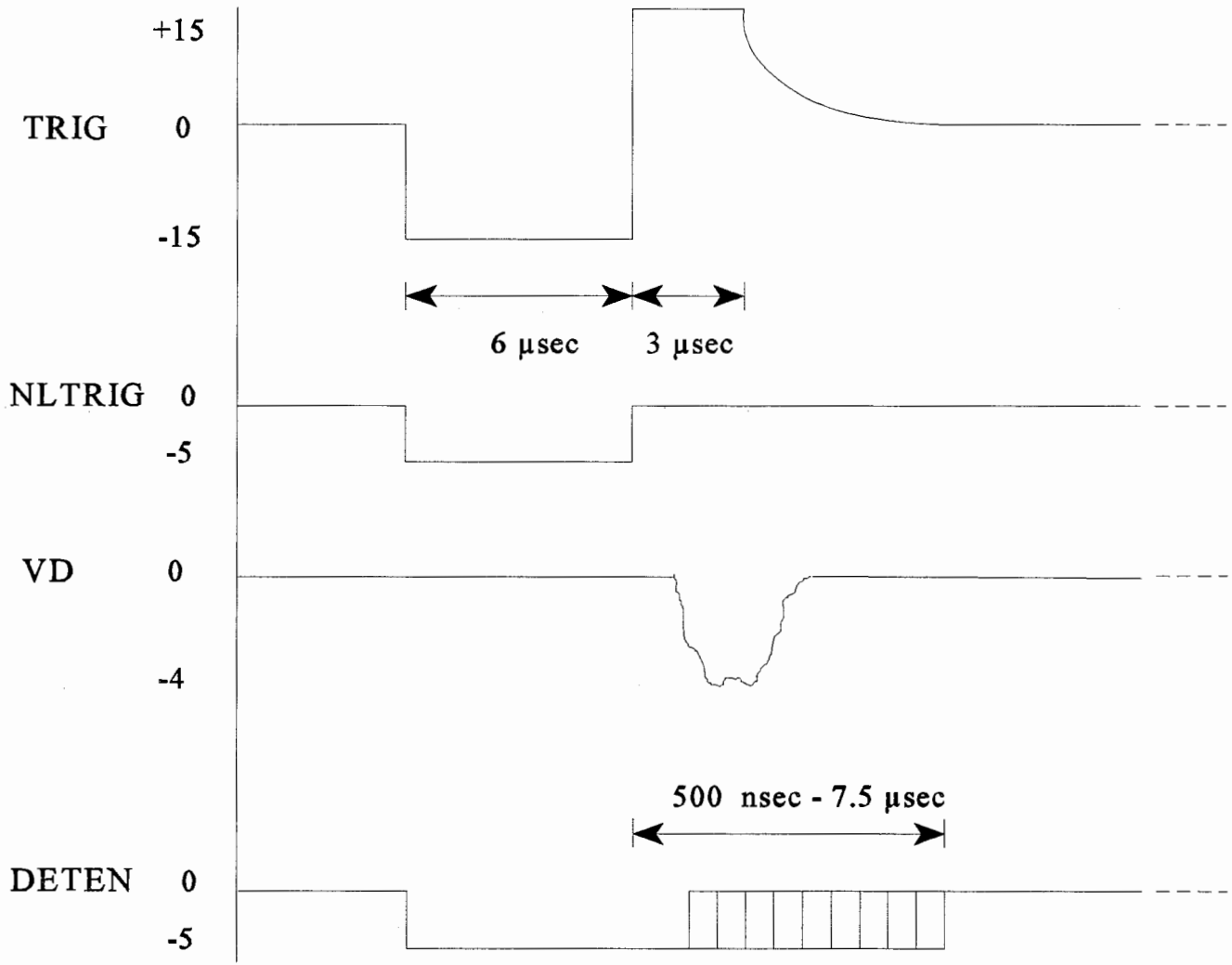

Figure 4.9 Timing diagram of TRIG, NLTRIG, VD, and DETEN. DETEN is used to blank out switching noise on the return signal line. DETEN is activated when NLTRIG rises to 0V.

4.4.2 Thresholding Function

The thresholding device is where the target detection and shutdown process occurs. The threshold subgroup produces the signal LSRCHK (LaSeR CHecK) that, when high, allows operation of the laser. When LSRCHK is low, the laser will stop firing. The thresholding circuitry is presented in Figure 4.10. This circuit is set to turn off the laser upon two consecutive detections of targets passing through the radar beam. The thresholding circuitry waits until DETEN goes high to detect aircraft.

The received signal after transmission, VD, is biased to a positive voltage level and passed through a low pass filter to remove any trace noises on the signal. This filtered version of VD, called VSIG, is one input to a voltage comparator that will determine if there is a legitimate target. The steady state of VSIG is 2.5V with any target detections represented as negative voltage returns. The maximum VSIG voltage magnitude is 2V. The reference voltage, VREF, can be adjusted from +2V to +0.4V through a potentiometer. Since the maximum signal return on VSIG has a magnitude of 2V, any thresholds set at 0.4V to 0.5V would never be crossed. Therefore, the laser would never be disabled, even though an airplane may have been detected.

Whenever the threshold is exceeded (VSIG falls below VREF), a target has been detected and the comparator output, THEX (THreshold EXceeded), rises to a logical one as long as VSIG is below VREF. When THEX goes high, a flip flop is reset and the inverted output (a logic one) is sent to the shift register when the radar cycle ends. When there are two detected targets in two subsequent cycles, LSRCHK will go low, shutting off the laser. Two target detections are required to eliminate laser shut down from false

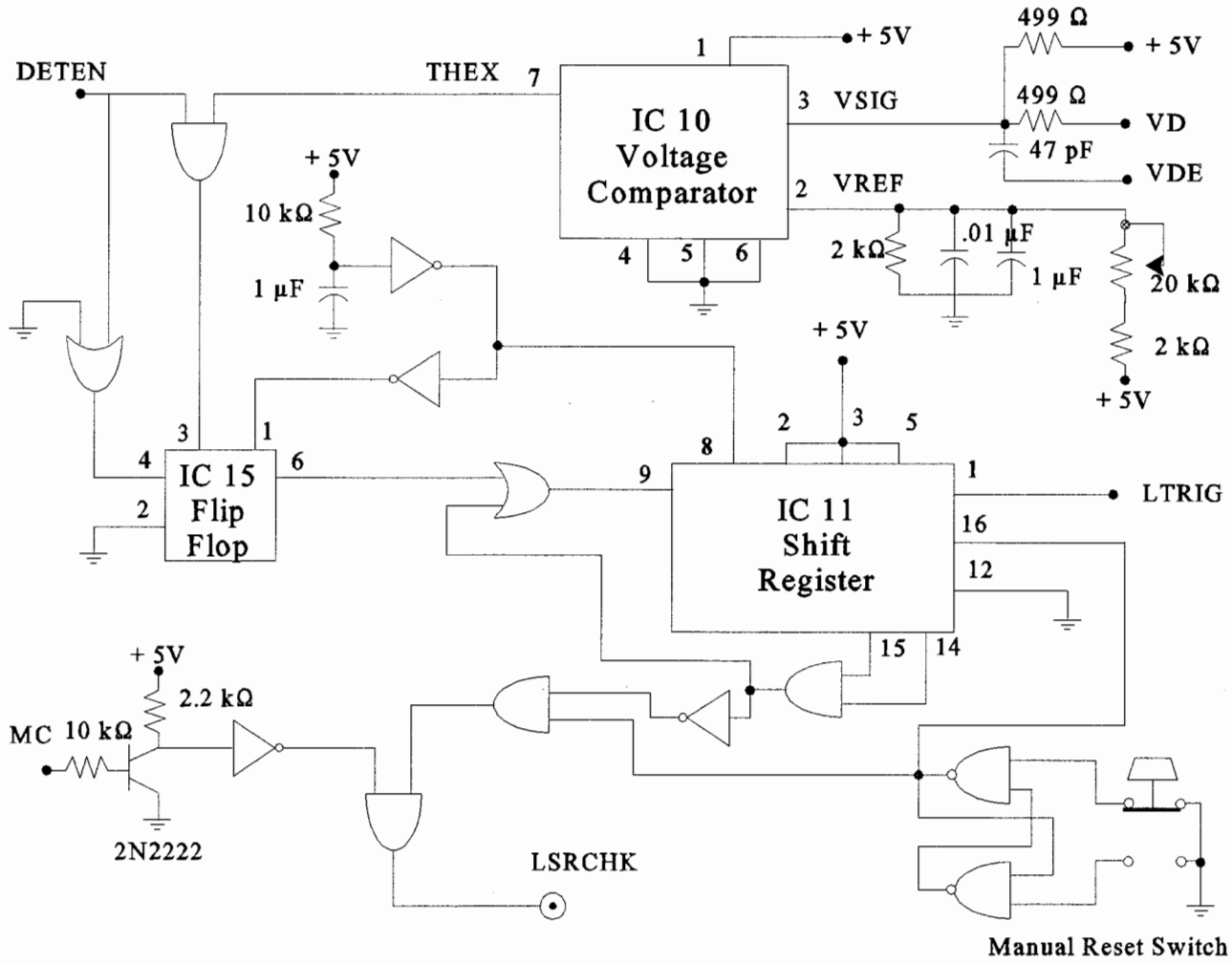

Figure 4.10 Thresholding circuitry for laser cutoff. The circuit disables the laser's Q-switch when two detections have been registered. Drawing is adapted from [19].

detections that would occur from the noise on the signal line.

Before LSRCHK is sent to the laser, it must pass one logic gate that was set up as a safety feature for accidental radar power failures or power shutdowns. The signal line, MC, from PC404 was used in the original motor for the R72. MC measures 0.6V when the radar is in stand-by mode and 8.9V when the radar is transmitting. Biasing to TTL level outputs, MC is low when in stand-by and high when transmitting. Thus, whenever the radar is placed back into stand-by mode or powered down completely, the logic of the AND gate will always set LSRCHK low and disable the laser. This additional safety interlock was not present on the LAMP laser cutoff circuit. Without this interlock, a safety hazard could easily occur if the radar were accidentally taken off line.

4.5 Monitor

The display monitor itself posed no limitations to the LARS system because it could be located alongside the electronics rack inside the LARS trailer and still receive information from the transceiver. On the other hand, the display monitor was designed to be used with a rotating antenna array and contained many functions that were only useful for maritime navigation. If only the basic functions of the radar were kept, such as tuning controls for transmitter and receiver sensitivity, a simple electronics chassis could be used instead of the display monitor. The signals generated by the radar could then be displayed on an oscilloscope to alert the user to various outputs.

The R72 display monitor contains the following printed circuit boards; PC401 (main control), PC402 (control panel), PC404 (terminal board), PC501 (power supply),

and the CRT display assembly (CML-286). By keeping only the necessary circuits for operation, these could be placed in a working arrangement in a small chassis box of about 7" height, which could mount in the standard 19" electronics rack with the other equipment. For this reason, circuit boards PC401, PC402, PC404, and PC501 were removed from the display monitor. CML-286 was not removed because an oscilloscope will be used instead of a CRT display.

4.6 Control Panel

The R72 control panel contains thirty functions dealing with the detection of other boats or other maritime obstacles. With the modification of the R72 system, many of those functions would never be used on LARS. Of the thirty functions, only six were deemed necessary for LARS operation

The functions of the new control panel are: STAND-BY mode, TRANSMIT mode, TUNE, GAIN, GROUND CLUTTER, and RAIN CLUTTER. Two momentary contact pushbutton switches are used to place the radar in the STAND-BY or TRANSMIT modes. Variable potentiometers are used for the others. TUNE is used to adjust the receiver to maximize target returns on VD. GAIN controls the gain of the receiver. GAIN increases or decreases the strength of the signal and noise on VD. GROUND CLUTTER and SEA CLUTTER reduce the gain of the receiver. GROUND CLUTTER can be used to suppress noise on VD. RAIN CLUTTER can be used to suppress echoes on VD from rain or snow.

A small printed circuit board was designed to accommodate these controls. It

measures 4.75" L x 3" W. This control panel has connections to both PC401 and PC501. If the operator desires, the old control panel (PC402) can be used on LARS simply by disconnecting the two input plugs and reconnecting PC402 to the system. A schematic of the printed circuit board making up the control panel can be found in Figure 4.11.

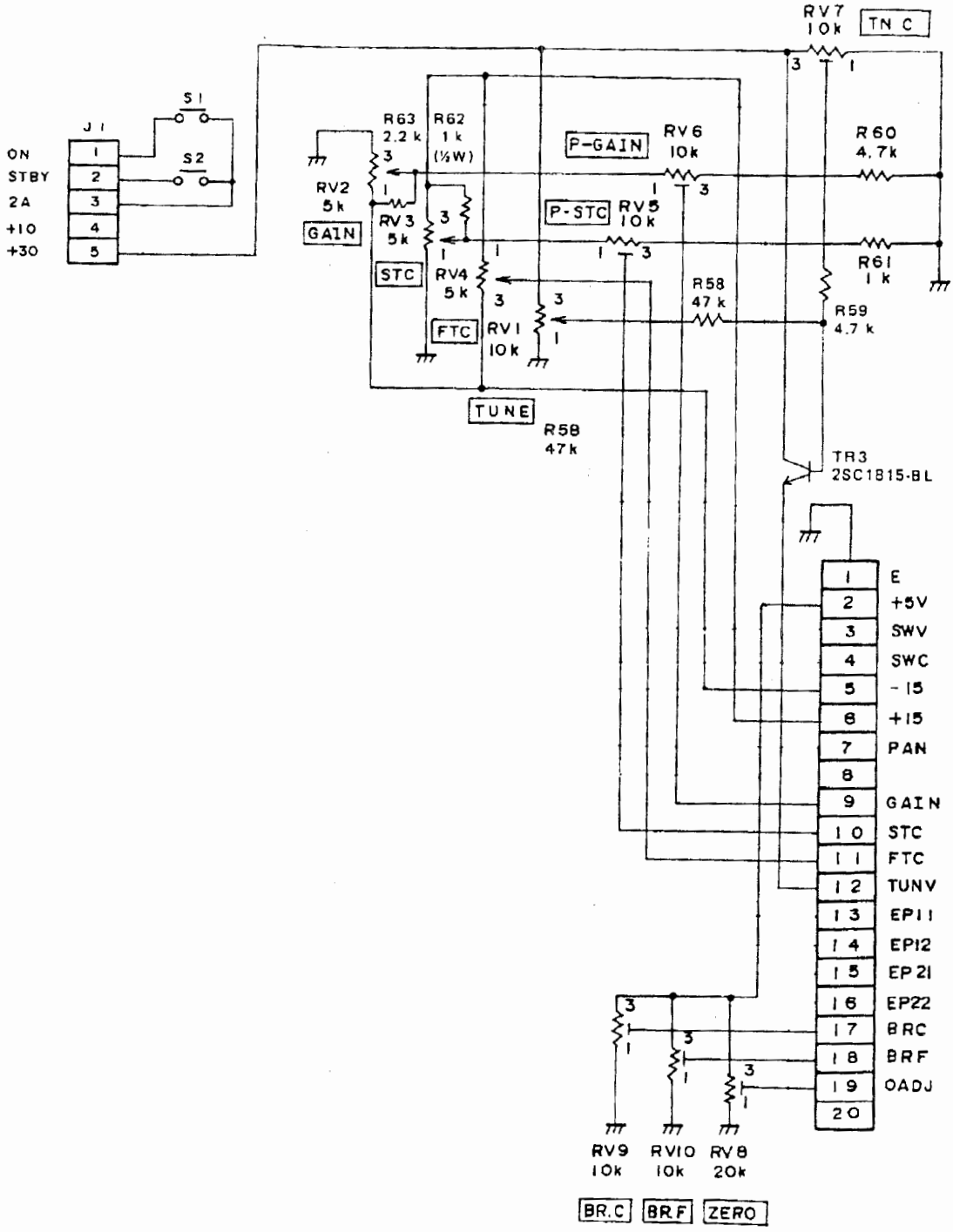

Figure 4.11 Control panel circuitry for the electronic chassis rack. This circuitry was adapted from the schematic of the R72 display monitor control panel [17].

Chapter 5

Safety Radar Components

The physical layout of the components is important to the overall design of the safety radar. With a project goal of streamlining the original system, much time went into designing a layout of all components to keep things simple yet functional. This chapter describes the setup of all the components that make up the rack mounted chassis. It also specifies the placement of the transceiver and antenna on the optical table.

5.1 Electronics Chassis

The electronics chassis is where all of the controls and circuitry are located. The chassis is contained in a standard 19" electronics rack inside the trailer with the LARS data acquisition equipment. The chassis measures 17.2" L x 17" W x 7" D. It has a solid bottom with a ventilated top cover. Side panel holes allow mounting of components. The chassis is fitted with slides and handles to allow the operator to examine the layout of the system. Friction disconnects permit the complete removal of the chassis from the rack. A picture of the chassis with the component placement is shown in Figure 5.1.

5.1.1 AC/DC Power Supply

The AC/DC power supply is a TrippLite 120VAC / 12VDC 25 Amp supply. It is mounted on the back left of the chassis. This supply was used because it was available in the PSU Lidar Laboratory at the time. During normal operation, the radar requires 5

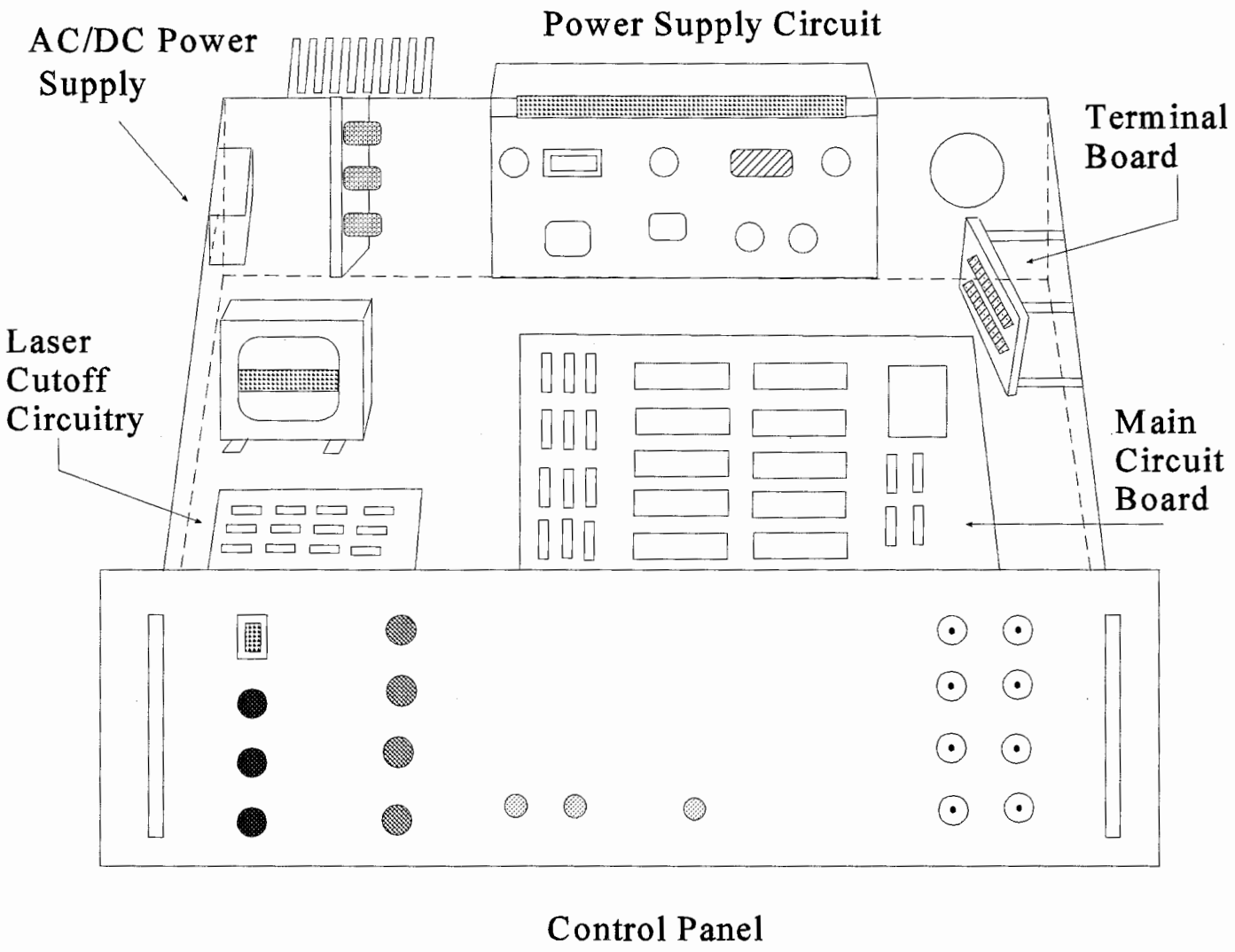

Figure 5.1 Electronic chassis layout. This figure shows the components that make up the electronic chassis of the safety radar system.

Amps for STAND-BY mode and 6.3 Amps for TRANSMIT mode.

5.1.2 Power Supply Circuit

The power supply circuit, PC501, is located on the back plane of the chassis. It was mounted standing up to allow a heat sink to be mounted on the outside of the chassis. The heat sink was bolted to the chassis for support. The transistors are connected to the heat sink by a half inch aluminum block. A notch was cut in the back plane to support the aluminum block. A small notch was cut into the top cover as well because the height of PC501 with the transistors is slightly over 7". Spacers were used in between the circuit board and back plane to support the board.

5.1.3 Main Control Circuit

The main control circuit, PC401, is mounted on the floor of the chassis. This board is where the video signal from the receiver is filtered, converted to a digital signal and stored in memory until called forth to be displayed. The control of all systems in the radar are routed through this board.

5.1.4 Terminal Board

The terminal board, PC404, is mounted on the right hand wall next to the 24 pin connector. It is mounted on braces to allow room for wires and plugs to be connected on the back of the board. The purpose of this terminal board is to act as a signal transfer/test point between the transceiver on the optical table and the main control circuit.

5.1.5 Laser Cutoff Circuitry

The laser cutoff circuitry is located near the front of the chassis on the left, directly in front of the AC/DC transformer. It was placed here to allow easier access to the potentiometers and the dipswitches on the card. The card is mounted on four standoffs to allow clearance for the wirewrap posts. The circuit receives its power from a +15V point on PC404. The +15V is connected to a 7805 +5V regulator on the circuit board to provide the power necessary for operation.

5.1.6 Control Panel

The front panel of the electronics chassis is where the controls for operating the radar are located as well as the signal outputs for shutting off the laser. The AC/DC power switch is located in the upper left corner. It is a lighted rocker switch to alert the operator when the system has DC power available to it. Beneath the AC/DC switch are three fuse holders. The top one is a 6 Amp fuse for the AC/DC power supply. The middle one is a 15 Amp fuse for the radar. The third fuse block is not in use. If a system is installed to the motor power jack on PC501, this fuse block could be used with that system. To the right of the AC/DC power switch are the four controls for the scanner. They are, from top to bottom, TUNE, GAIN, GROUND CLUTTER, and RAIN CLUTTER.

In the middle of the control panel are the STAND-BY and TRANSMIT controls. The STAND-BY button is black while the TRANSMIT button is red in case the labels can not be seen by the operator due to low light, viewing angle, etc. In addition, the RESET

switch for the laser cutoff circuitry is located to the right of the TRANSMIT button. It is black so it is not confused with the TRANSMIT button.

On the right hand side of the front panel are eight BNC connectors which provide signals to monitor the radar's performance. Of the eight, six are currently in use. A summary of the eight outputs is shown in Figure 5.2.

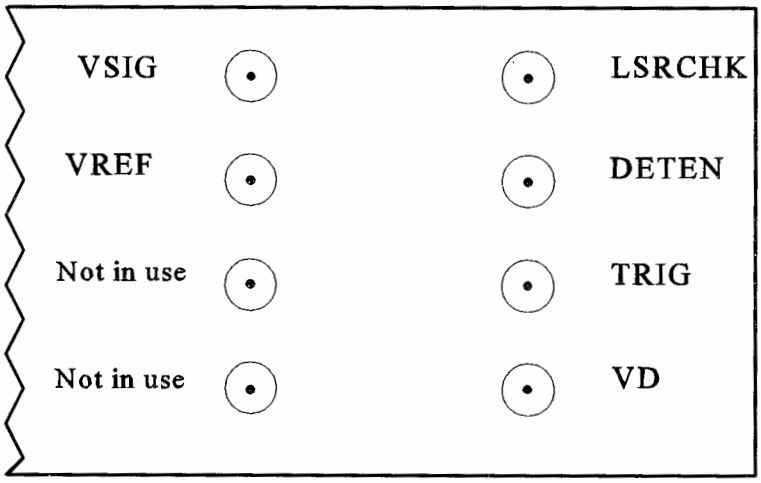

Figure 5.2 BNC outputs available on control panel

Two BNC outputs are not currently used but are available if the operator would want additional signals on the front panel. LSRCHK contains the signal for shutting down the laser and must always be connected to the data acquisition circuitry for disabling the laser's Q-switch.

5.2 Transceiver and Antenna

The safety radar transceiver and antenna will be mounted on the laser side of the table. Enough room was allowed to let the stepper motors of the motorized mirror fit without crowding both systems. The scanner is fastened to the optical table by bolts through the mounting plate. The 10 meter interconnection cable plugs into the back of the unit and leads down one of the forks of the optical table so the cable does not interfere with the movement of the table. With the modifications, the transceiver with antenna now weighs 22 pounds, that is 28 pounds lighter than the original hardware.

The antenna is mounted onto the optical table by two horseshoe shaped plates. One plate is used to hold the antenna. The second plate is a little longer and mounts to the optical table. Each plate has three tapped holes and three clear holes with six cap screws separating the two plates by one half inch. Because mounting the antenna to the optical table may not align the beam pattern with the laser, the antenna had to be able to move slightly so the radiation pattern of the antenna could fully enclose the laser beam. If possible, the laser should pass through the center of the radiation pattern. The six cap screws, by tightening and loosening them in sequence, can move the antenna up, down, left, or right. The antenna has two degrees of freedom in the vertical and horizontal directions due to the plate spacing and the tolerances of the holes.

A rifle scope was added to the antenna mounting plate for laser-antenna alignment. With the scope, the antenna can be moved to provide full coverage around the laser beam by aiming the antenna through the scope. The scope also allows the antenna to be pointed at a particular object to determine signal strengths. A side view of the transceiver/antenna

setup is found in Figure 5.3. Figure 5.4 shows the placement of the safety radar on the optical table.

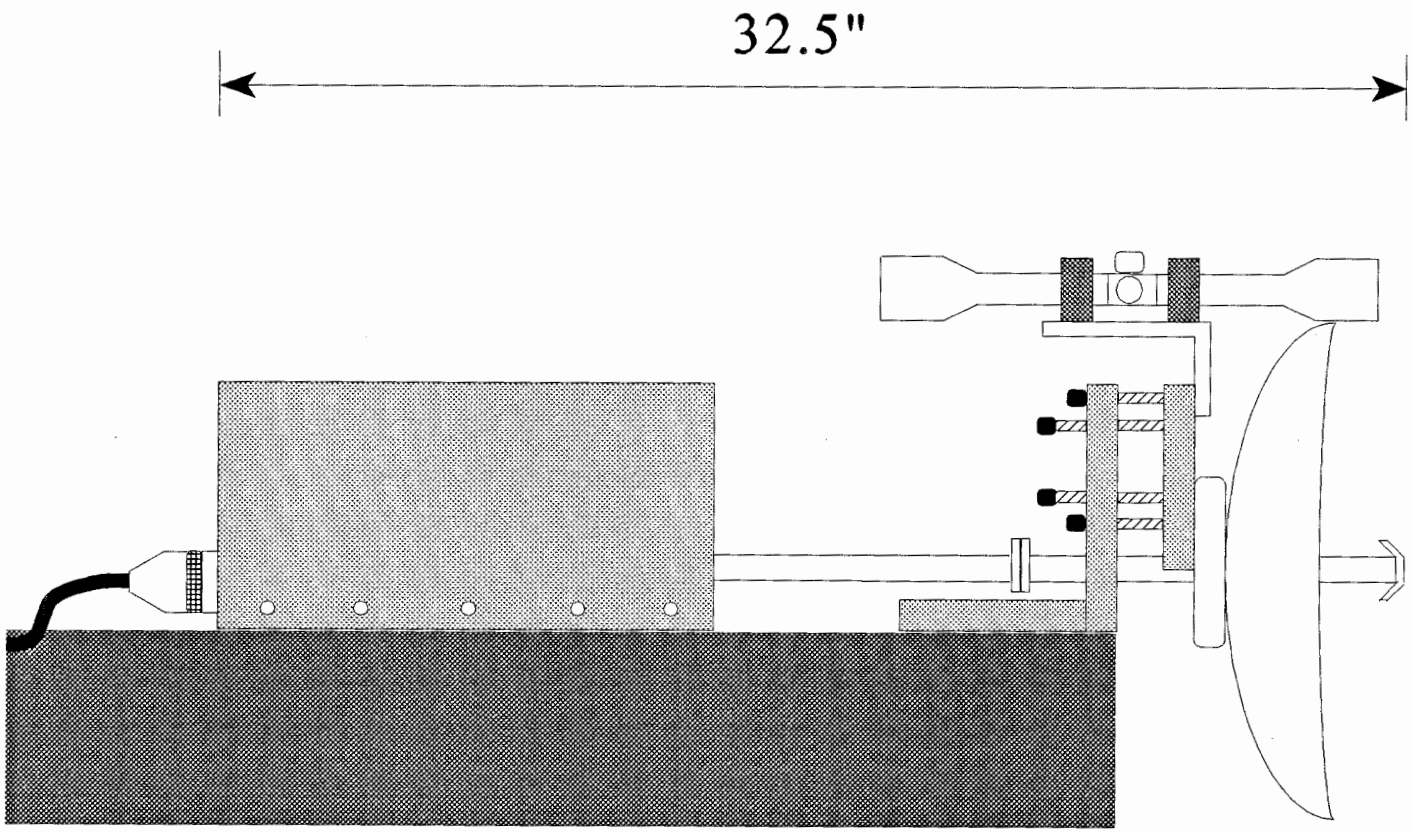

Figure 5.3 Side view of transceiver housing with antenna on optical table. The length of the transceiver with antenna is 32.5 inches. The weight of the combined units is 22 pounds.

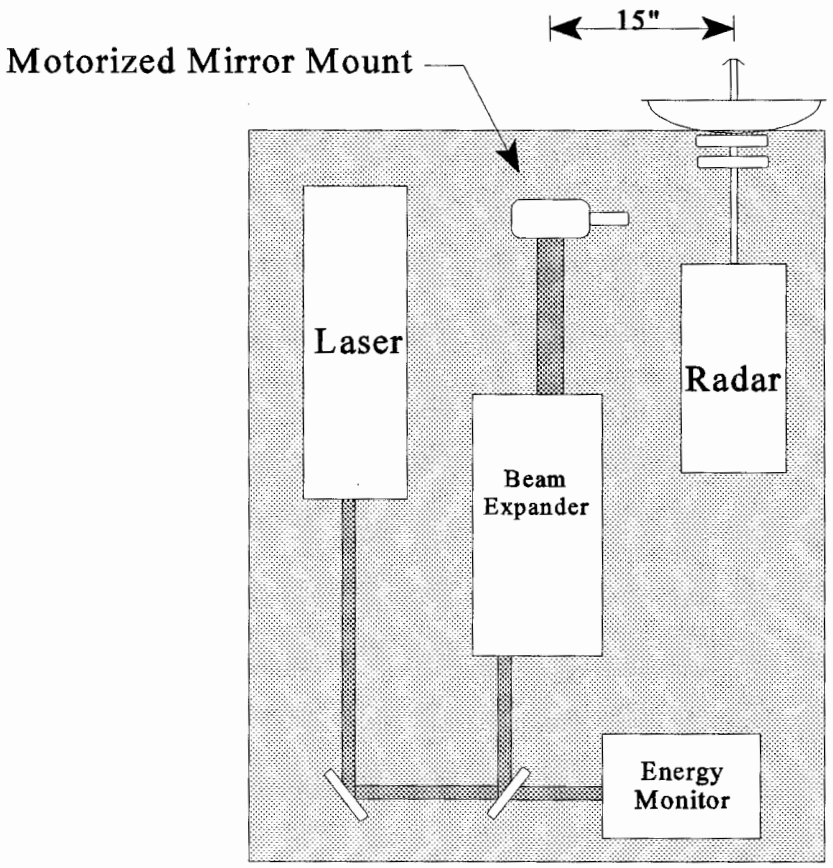

Figure 5.4 Bottom view of the LARS optical table. This diagram shows the placement of the radar system from the laser beam.

Chapter 6

Testing and Evaluation of the Safety Radar System

The testing of the radar system is important to verify that the radar will indeed shut off the laser when an aircraft approaches the beam. Before installation on the optical table, the radar was tested against a variety of targets to determine return signal characteristics. The signal was analyzed to determine if the radar will be able to detect aircraft and to point out any potential problems with the laser cutoff system.

6.1 Radar Range Equation

The radar range equation is used to characterize the return signal from a radar transmitter. The received signal is a function of how much energy was transmitted, what scattered the energy, and the effective areas of the transmitting and receiving antenna.

Assuming the transmitting and receiving antennas are pointed at a target, the power density incident on the target is,

$$S = \frac{P_t A_t}{\lambda^2 r^2}$$

where, S - Incident power density (W/m^2),

P_t - Transmitted power (W),

A_t - Effective area of the transmitting antenna (m^2),

λ - Transmitting wavelength (m),

r - Distance from antenna to target (m).

The power incident on the target is proportional to the power density and is written as,

$$P = \sigma S$$

where, P - Power reradiated by target (W),

σ - Radar cross section (m^2).

The power density arriving at the receiving antenna, because it is assumed the target is reradiating the power isotropically, is written as,

$$S = \frac{P}{4\pi r^2}$$

The power seen at the receiving antenna terminals is then,

$$P_R = A_R S$$

where, A_R - Effective area of receiving antenna (m^2).

Combining these equations, the resulting formula is known as the radar range equation,

$$P_R = \frac{P_T A_T A_R \sigma}{4\pi r^4 \lambda^2}$$

If the transmitting antenna and the receiving antenna are the same, $A_R = A_T$. The radar range equation could also be written in terms of gains G_T and G_R. Again if the same antenna is used to transmit and receive, $G_T = G_R = G^2$. The radar range equation in terms of gain is written as,

$$P_R = \frac{P_T G^2 \lambda^2 \sigma}{(4\pi)^3 r^4}$$

6.2 Analysis of Safety Hazards for the Safety Radar

An analysis of the LARS safety radar system was performed to determine the potential hazard areas. The two types of hazards are electrical and exposure to radio frequencies from the antenna. The electrical hazard is the high voltages generated by the system to power the transmitter. There are several locations in the chassis and scanner where +360V is available. If work must be performed on the chassis or scanner, an entire system shutdown is recommended. Because all of the circuit boards are within close proximity of each other, a tool or loose wire can easily short out a system.

The guidelines concerning the safety from exposure to the electromagnetic radiation was taken from the American National Standard (C95.1-1982). For the safety radar operating at 9.4 GHz, the power density of the radiation coming from the antenna is 50 W/m^2 [21]. To determine the safe area around the antenna, the following equation was used,

$$\frac{10\ kW * Gain}{4\pi r^2} = 50\ W/m^2$$

where, r - Recommended safe distance (m).

According to the calculation, r = 116.39 meters (381.85 feet). This safe distance was

calculated along the center line of the antenna. Since LARS can only scan down to 30° elevation, the chance of the antenna pointing directly at a person is extremely unlikely.

6.3 Aircraft Detection Abilities

The radar range equation lists as one of its variables the radar cross section of the intended target. This cross section is an important number for LARS because it is a scanning lidar system. The most common profiles that the radar could see are a nose view, side view, and bottom view of an aircraft. The radar cross sections of typical aircraft that LARS may encounter are given in Table 6.1.

Table 6.1 Radar Cross Sections of Typical Aircraft [22]

	Nose View (m^2)	Broadside View (m^2)
Small Commercial Plane	0.2 - 10	5 - 300
Midsize Commercial Jet (ex. Boeing 727)	4 - 100	200 - 800
Large Airline Jet (ex. DC-8)	10 - 500	300 - 550

The cross sections vary on each aircraft for the different views because the cross section is affected by area and reflection angles. Although Table 6.1 lists only the nose and broadside view cross sections, it would be safe to assume that the bottom view of an aircraft, with its larger area, would have a large cross section.

Another factor in aircraft detection is the receiver sensitivity. The receiver of the safety radar is specified to -102 dBm. However, it is expected that the actual signal to

noise ratio (SNR) needed for positive detection of aircraft to be above the minimum based upon previous use of safety radar systems [2]. In order to find the actual SNR, the following cross sections were assumed and are located in Table 6.2.

Table 6.2 Cross Sections and Received Power for Typical Aircraft

		Nose View		Broadside View	
Plane	Altitude	Cross Section	Received Power	Cross Section	Received Power
Small	10,000 ft (3048 m)	1 m^2	-73.6 dBm	200 m^2	-50.6 dBm
Midsize	30,000 ft (9144 m)	50 m^2	-75.7 dBm	350 m^2	-67.3 dBm
Large	35,000 ft (10668 m)	250 m^2	-71.4 dBm	425 m^2	-69.1 dBm

The hazard zones of the laser must be calibrated against the detection zones of the radar. When the laser and safety radar are zenith pointing, the radar must be able to detect aircraft up to its maximum altitude. The SNR cannot be set from the zenith pointing position however. When the laser scans down to a 30° elevation angle, the detection zone falls short of the laser's hazard zone. Thus, the SNR must be determined at the lowest elevation angle possible.

The radius of the radar's detection zone was calculated at 30° elevation angle using a nose view of the medium size aircraft since it produced the lowest received power. As a worst case assumption, the altitude of the large jet was used. For a medium size jet, the detection zone of the radar must extend out to 23.34 km, which corresponds to -92 dBm. Therefore, based upon the received minimum sensitivity of -102 dBm, the SNR of the

radar will be 10 dB above the minimum. If a margin greater than 10dBm is selected, then the minimum elevation angle can be raised to correspond to this value. Figure 6.1 shows the calculated detection zone for the radar.

Because two sequential detections are required for laser shutdown, we must verify that a plane could not cross through the beam pattern of the radar and contact the laser beam before the cutoff circuit has disabled the Q-switch. As a worst case, the beam edge to center distance was calculated for a small plane flying at 1000 feet. The time needed for laser cutoff was taken to be three times the pulse repetition frequency of the radar to insure an adequate margin of safety. This distance along with the velocity is shown in Table 6.3. Since a small aircraft will not approach this speed, this shows that the safety radar approach is valid.

Table 6.3 Beam Edge to Center Distances

Aircraft	Altitude	Edge to Center Distance	Intercept Velocity
Small Plane	1000 ft.	213.75 ft.	36, 527 mph.

6.4 Testing of System

The testing of the safety radar was carried out in locations where fixed and moving targets were available. One such location where the safety radar was tested was the Applied Research Laboratory's Steam Facility located near the University Park Airport. This location provided fixed targets in the form of mountain ranges as well as the chance

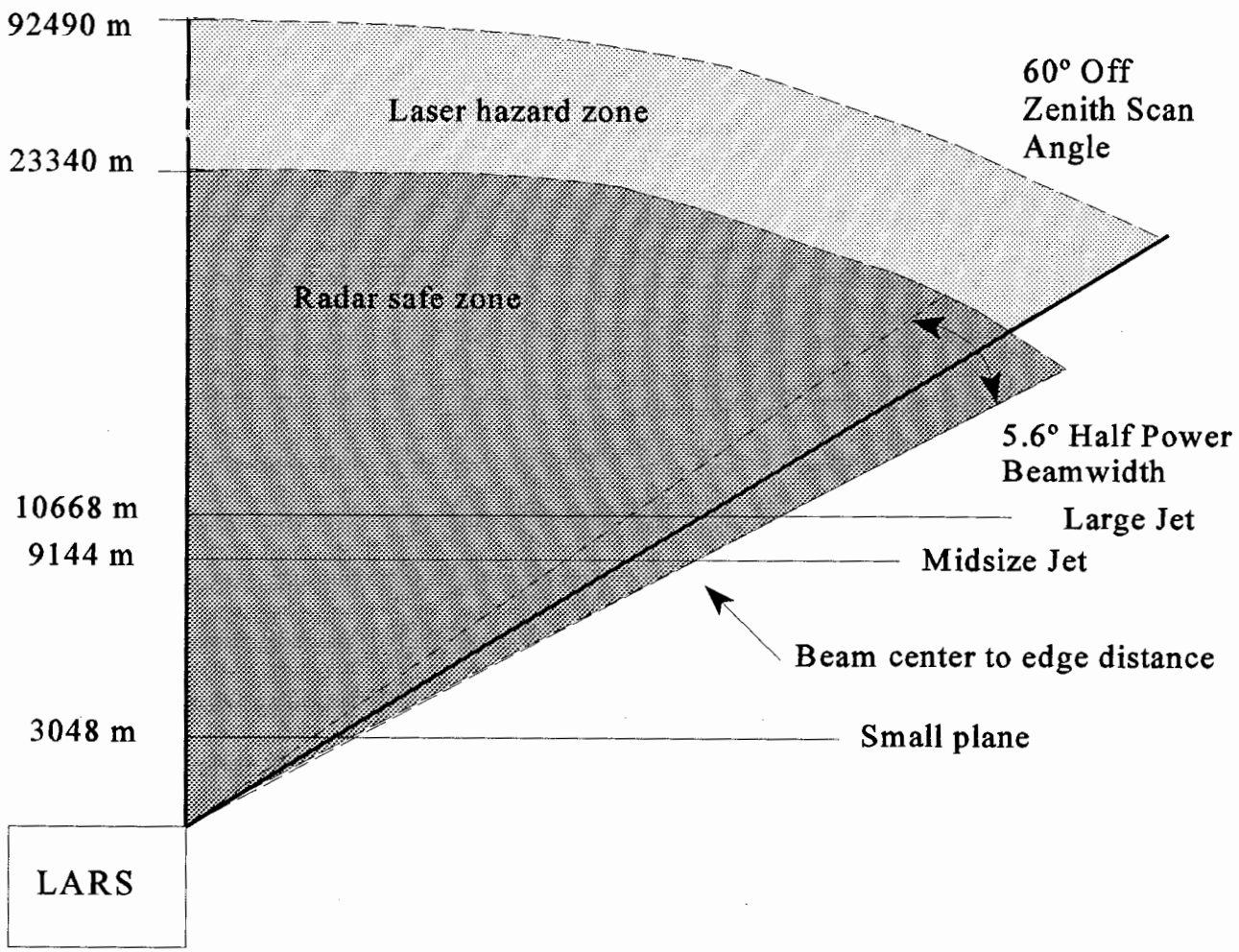

Figure 6.1 Calculated detection zone for the radar. This figure shows how the radar encompasses the laser to protect aircraft.

to detect aircraft flying in or out of the airport.

The scanner unit with antenna was mounted on an adjustable telescope tripod. Testing was carried out by two people, one to aim the antenna at targets through the scope while the other monitors the return signal on a Hewlett Packard 54502A digital oscilloscope. This two person team allowed a continuous tracking capability to determine how far aircraft can realistically be detected.

The system tests were conducted with a receiver SNR of -92 dBm. The pulse repetition frequency (PRF) was set at 750 Hz. The radar system itself has an adjustable PRF ability with a range of 500 Hz up to 2000 Hz. However, the 750 Hz PRF has been chosen for operation because it delivers the most power during the transmitted pulse. The average power was determined by multiplying the peak power, PRF, and pulse length together. Table 6.4 shows the average power delivered by each setting.

Table 6.4 Average Power Delivered by Radar for Various PRF

PRF (Hz)	Pulse Length (μsec)	Average Power (W)
2000	0.08	1.6
1500	0.25	3.75
750	0.7	5.25
500	0.7	3.5

6.5 Return Signal Analysis

The signal analysis consisted of studying the waveforms that were plotted from the

oscilloscope. The signals were examined to determine the distances to the detected target and the return signal strength. The display monitor from the R72 system was used to help verify the returns of the system. The old display monitor was reconnected to PC401 through the CRT display assembly (CML-286.) The display monitor has a variable range marker function available on the old control panel that can determine how far an object is from the antenna. This function was especially helpful with fixed targets to compare what the display monitor calculated to what the oscilloscope displayed.

Three separate aircraft were detected by the radar. In each case, the targets were small commuter planes flying broadside to the testing area. For all three return signals, each crossed the cutoff circuit threshold and would have shut down the laser. Table 6.5 lists the results of the three aircraft. The plots of VSIG are found in Figures 6.2, 6.3, and 6.4 respectively.

Table 6.5 Results of the Safety Radar Tests

Figure	Target	Distance to Target	Received Power	Threshold
6.2	Small Plane	7.35 km	-65.9 dBm	-39.54 dBm
6.3	Small Plane	5.25 km	-60.1 dBm	-22.54 dBm
6.4	Small Plane	6.75 km	-64.4 dBm	-34.5 dBm

6.6 Error Analysis for Signals and System

There are three factors that could affect the return of the reflected signal. They are the radar cross sections, attenuation from the atmosphere, and operating temperature.

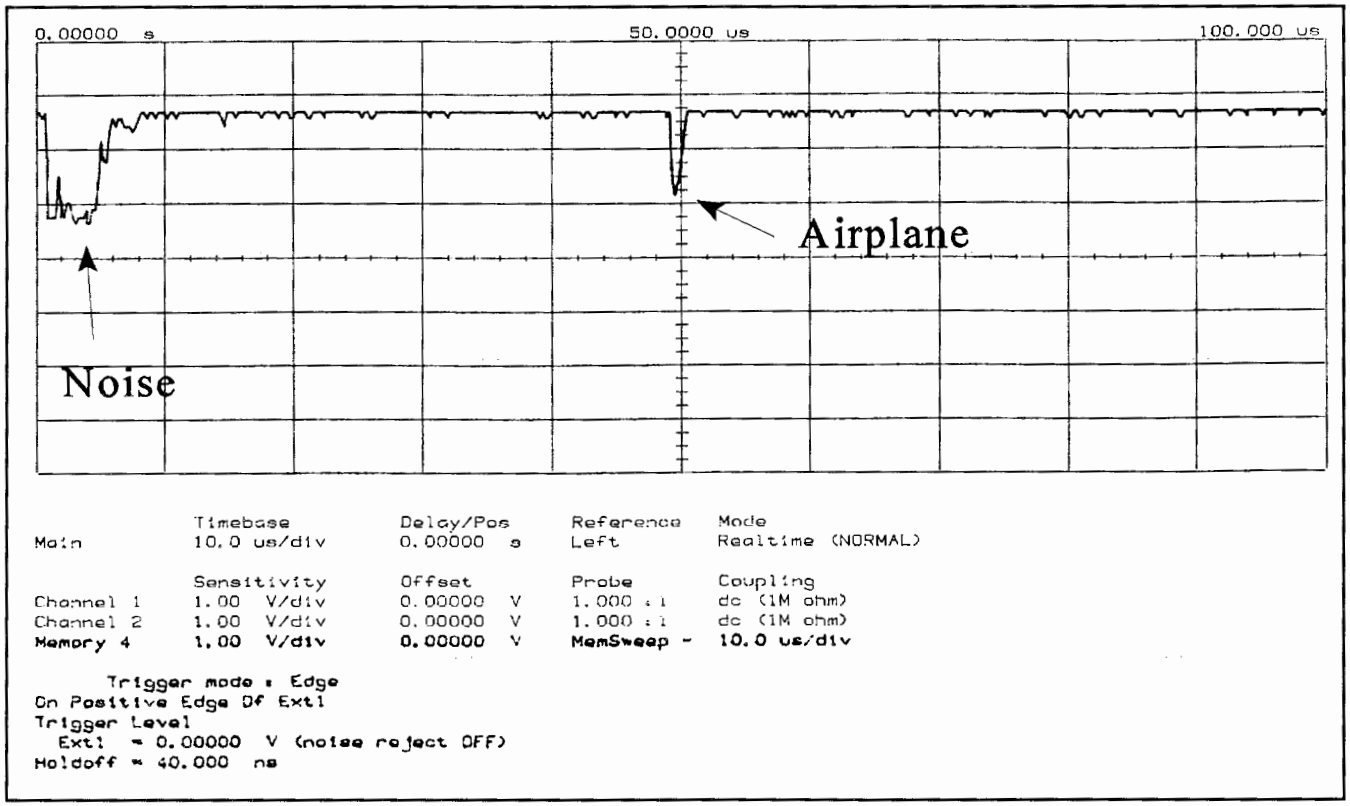

Figure 6.2 Result of radar test. This aircraft was detected at 7.35 km with a signal strength of -65.9 dBm.

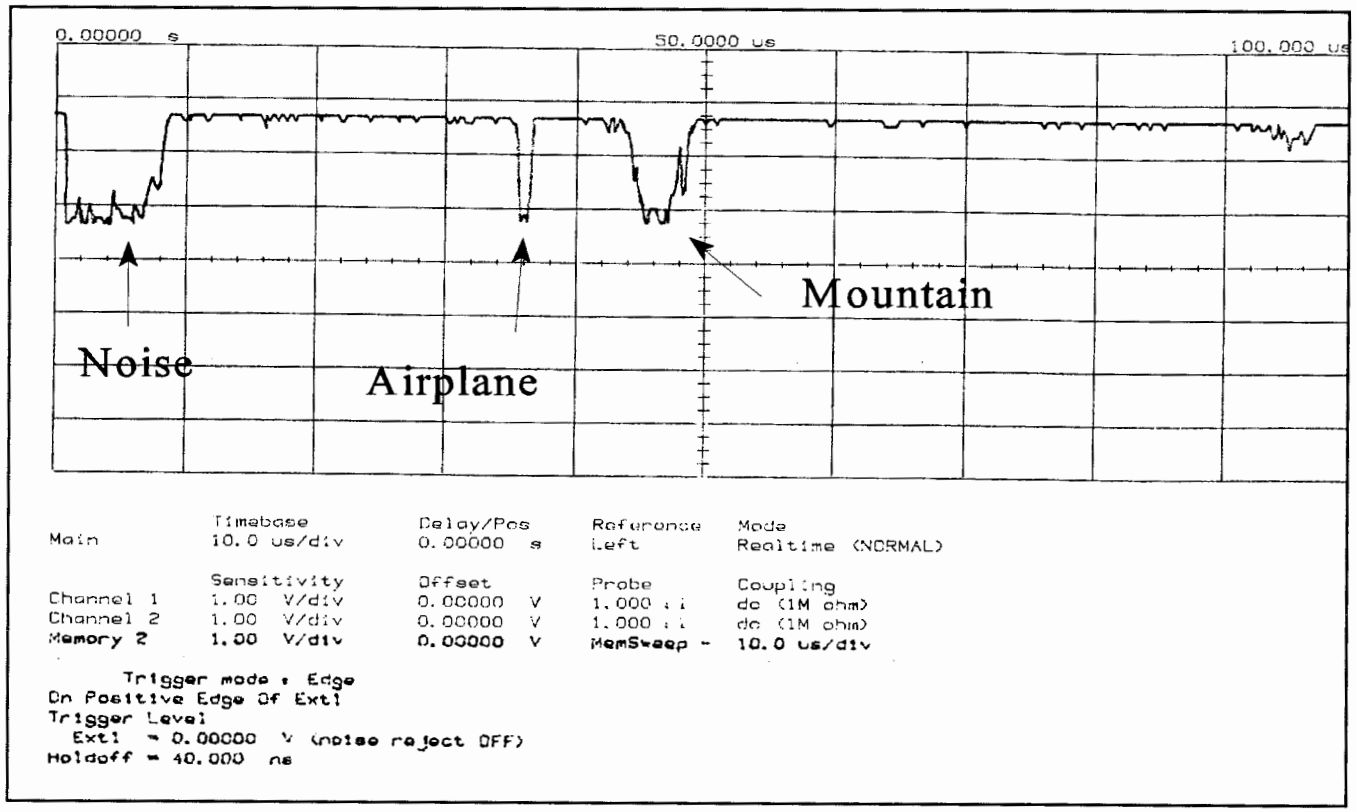

Figure 6.3 Result of radar test. This aircraft was detected at 5.25 km with a signal strength of -60.1 dBm.

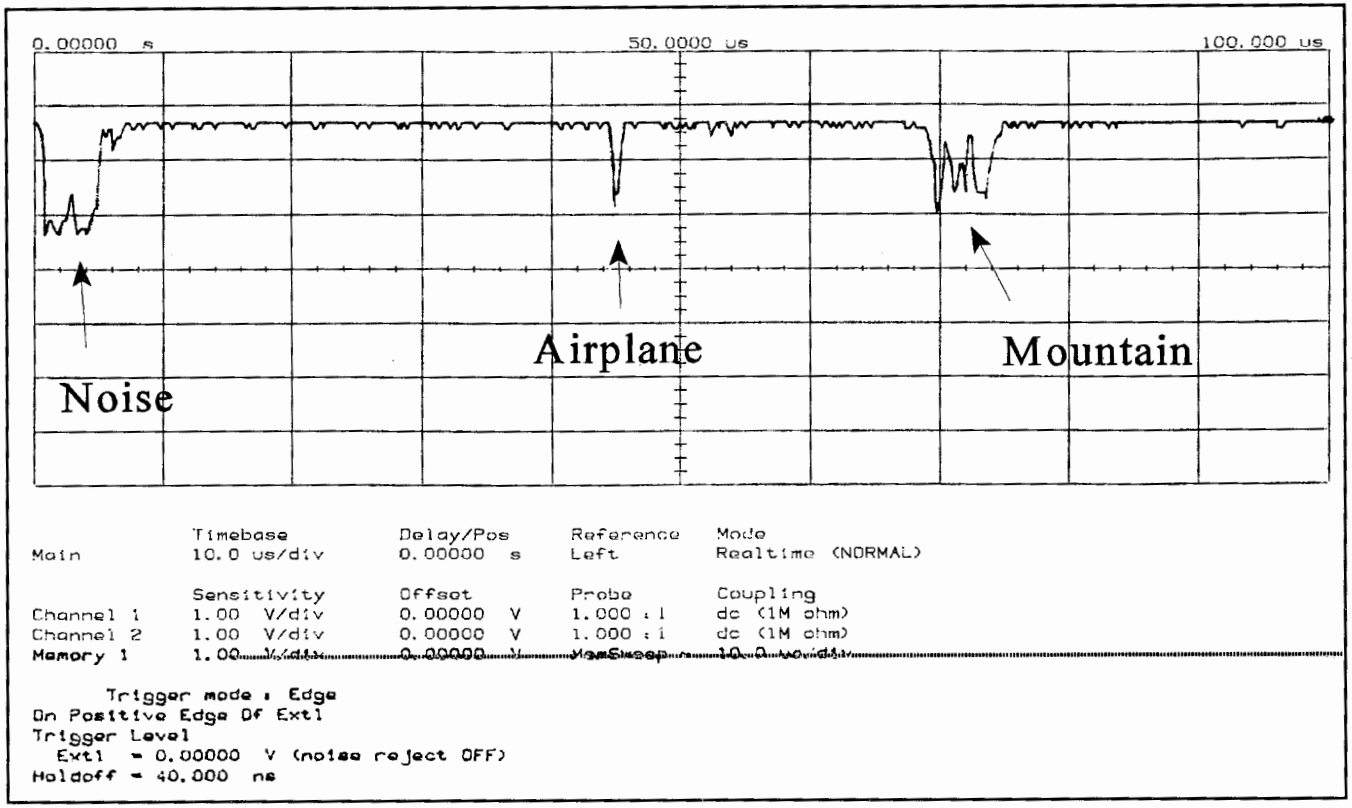

Figure 6.4 Result of radar test. This aircraft was detected at 6.75 km with a signal strength of -64.4 dBm.

The calculated detection range was based on an assumed cross section. However, aircraft are constantly moving and so their cross section changes. A weak return might be caused from a particular view angle of the radar. With the SNR set 10 dB above the minimum, the receiver will be able to detect small cross sections of aircraft.

In addition, attenuation due to the atmosphere can also affect the strength of the return signal. The radar is not free from attenuation at 9.4 GHz. Yet, the attenuation is slight enough that it can be disregarded unless LARS was operating in a heavy rainstorm. The tests performed here were taken in mostly clear skies with relatively few clouds. Attenuation due to the atmosphere would not have affected these signals.

Similarly, the operating temperature of the electronics can influence the noise on the signal line. The operating temperature of the transceiver is rated at -25° to + 55° C while the electronic chassis is rated for -15° to + 50° C [17]. With an increase in temperature, noise will likely increase on VSIG. However, LARS will most likely operate in temperature ranges between +10° to +30° C during measurement campaigns so noise will not factor into the signal return.

The parabolic dish antenna can also contribute to errors in the return signal. The first sidelobes are 10° off the main beam. The sidelobes are 23.5 dB down from the main lobe. In other words, each first sidelobe has 5.8 dB of gain. The antenna pattern is shown in Figure 6.5. Throughout a scan, there is a possibility that a sidelobe could pick up a target and would register it as a false detection. For a small aircraft flying at 10,000 ft broadside to the radar, the sidelobe would produce a return equal in magnitude to the main lobe only if the airplane was 668 ft away. Therefore, aircraft false detections from

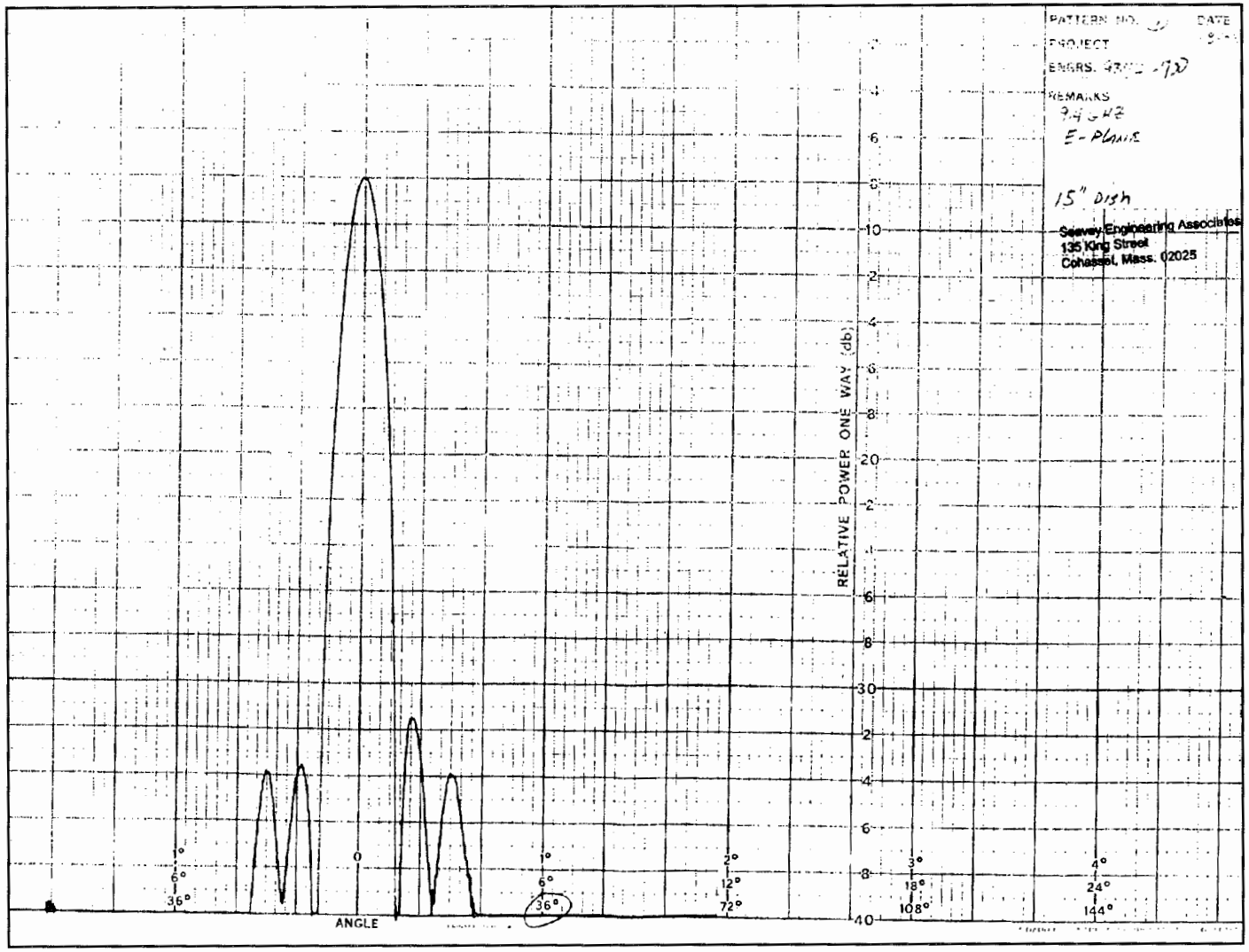

Figure 6.5 Beam pattern of the safety radar antenna. The sidelobes are 23.5 dB down from the main lobe [18].

the sidelobes are minimal at best. The sidelobe problem could also mean false detections from tree lines or buildings when at 30° elevation angle. If this were to occur, the elevation scan angle could be raised to the point where no false detections occur .

6.7 Signal Stability

Since the detection zones of the radar were calculated based on the transmitted and received power, the transmitter and receiver should be checked periodically to assure signal stability. The transmitted power can be measured with a radar test set calibrated to 9.4 GHz. The sensitivity of the receiver can be checked with a small target of a known cross section. By placing the target one kilometer from the radar, the received power can be verified. These tests would be performed in monthly intervals by LARS personnel and the results kept in a logbook inside the mobile laboratory.

6.8 Future Work

The safety radar that has been presented here is by no means an optimized system. Several components can be improved further such as the laser cutoff circuit. When the laser has been disabled by the cutoff circuitry, a reset button must be pushed to restart the laser. For a hands-off system, a cutoff circuit with an internal reset switch would activate when the radar no longer detects aircraft. With this capability, the operator is free to concentrate on other systems while the lidar follows a scan program.

As the work of the LARS progresses in the future, smaller elevation scan angles might be pursued. To achieve longer radar zones, a more powerful transmitter or

sensitive receiver must be acquired to expand the safe area outward. An antenna with higher gain could also help develop longer range safety scans.

A third area to be studied is when the receiver is swamped by transmission from another 9.4 GHz radar. By building a circuit to jitter the transmitted pulse, the detected returns can be gated to eliminate saturation from other marine radars.

These are only three future work questions that could be follow up projects for the safety radar. Any further hardware modifications to the system would only be for the benefit of the operator. With two BNC connections on the front panel and a power connection on PC501, the operator is encouraged to adapt the system to their needs.

Chapter 7

Conclusions

This thesis presented a safety radar system that was constructed to help complement spotters to detect aircraft during LARS operation. Since LARS has a scanning lidar system in its overall design, aircraft were liable to be illuminated by the laser at off zenith angles. Using a safety radar could extend the range of safe operation for LARS, protecting aircraft that might be hidden to spotters because they are behind clouds or fog.

An analysis of the optical hazard of the laser was presented to show why a safety system is needed to protect aircraft from the laser. A marine radar, with its small size and low cost, provided the essential makeup of the safety radar system. Through modifications, the radar was rebuilt with simple controls and a compact design. Circuitry was built to act as an interface between the radar and the laser to enable the radar to shut down the laser when an airplane approached the beam. Tests were performed to verify that aircraft will enter the operator set threshold region and will disable the Q-switch if the threshold were crossed. Sources of error were discussed along with future directions that the radar could take towards improvement.

References

1. Measures, R. M., Laser Remote Sensing. Florida: Krieger Publishing Co., 1992.
2. Philbrick, C. R., et al., "Measurements of the High Latitude Middle Atmosphere Dynamic Structure Using Lidar," AFGL-TR-87-0053, Environ. Res. Papers, No. 967, Hanscom AFB, MA, 18 February 1987.
3. Rajan, S., et al., "Aerosol Mapping of the Atmosphere Using a Multiple Wavelength Polarization Lidar," COMEAS Proceedings, 111-114, 1993.
4. Anuskiewicz, J., "A Volume Scanning System for a Lidar and Radar Sounder," MS Thesis, The Pennsylvania State University, 1993.
5. Mathason, B., "Performance Efficiency of the WAVE-LARS Scanning Lidar System," MS Thesis, The Pennsylvania State University, 1994.
6. Haris, P. A. T., "Performance Analysis of the LAMP Rayleigh/Raman Lidar System," MS Thesis, The Pennsylvania State University, 1992.
7. Philbrick, C. R., et al., "Lidar Measurements of Middle and Lower Atmosphere Properties During the LADIMAS Campaign," Proceed. 16th Intl. Laser Radar Conference, NASA Conf., 3158, pp. 651-654, 1992.
8. Philbrick, C.R., "Raman Lidar Measurements of Atmospheric Properties," Proceed. SPIE, 2222, pp. 922-941, 1994.
9. American National Standard for Safe Use of Lasers, ANSI Standard Z136.1-1993, Laser Institute of America, Orlando, FL, 1993.

10. Mihran, Richard T., "Interaction of Laser Radiation With Structures of the Eye," IEEE Trans. Education, 34, no 3, Aug. 1991, pp. 250-259.

11. Allen, Richard G., Labo, Jack A., and Michael W. Mayo, "Laser Eye Protection," Proceed. SPIE, 1207, 1990, pp. 34-45.

12. Sliney, David and Myron Wolbarsht. Safety with Lasers and Other Optical Sources. New York: Plenum Press, 1980.

13. Zuchlich, Joseph A., "Ultraviolet Laser Effects on the Cornea," Proceed. SPIE, 1207, 1990, pp. 48-58.

14. Continuum Operation and Maintenance Manual Surelite II-20, Santa Clara, CA.

15. CCIR Report 5/270, CCIR XIV Plenary Assembly, Kyoto, Draft Document 5/1024/E, November 23, 1977.

16. Interoffice Correspondence, LAMP Lidar Tests at Point Mugu: Final Report, 15 June 1994, Applied Research Laboratory, University Park, Pennsylvania.

17. Raytheon R72 Raster Scan Marine Radar Manual, Raytheon Marine Company, Hudson, N.H.

18. Interoffice Correspondence, Electrical Test Report, AS15-90 15" Diameter Antenna, Seavey Engineering Associates, Inc., Cohasset, MA.

19. Moyer, William W., Interoffice Correspondence SE93-200, Design of a LAMP Radar Safety Subsystem, Applied Research Laboratory, University Park, Pennsylvania.

20. Federal Aviation Regulations Revised Part 91: General Operating and Flight Rules, August 18, 1990, Federal Aviation Administration.

21. American National Standard Safety Levels with Respect to Human Exposure to Radio Frequency Electromagnetic Fields, 300 kHz to 100 GHz, ANSI Standard C95.1-1982, IEEE, New York, NY, 1982.

22. Blake, Lamont V. Radar Range-Performance Analysis. Massachusetts: Lexington Books, 1980.